In-Situ Electro Plastic Treatment for Thermomechanical Processing of CP Titanium

Mohammed Abdul Khalik
Swinburne University of Technology, CSIRO
Saden H Zahiri
CSIRO
Syed H Masood
Swinburne University of Technology
Suresh Palanisamy (spalanisamy@swin.edu.au)
DMTC, Swinburne University of Technology https://orcid.org/0000-0003-1597-8696
Stefan Gulizia
CSIRO

Research Article

Keywords: Titanium, Resistant heating, Thermomechanical treatment, Electro-plastic deformation, Recrystallization, Grain refinement

Posted Date: March 23rd, 2021

DOI: https://doi.org/10.21203/rs.3.rs-306405/v1

In-Situ Electro Plastic Treatment for Thermomechanical Processing of CP Titanium

Mohammed Abdul Khalik[1,2], Saden H. Zahiri[2], Syed H. Masood[1], Suresh Palanisamy[1,*] and Stefan Gulizia[2]

[1] School of Engineering, Swinburne University of Technology, Hawthorn, VIC, Australia,

[2] CSIRO, Clayton, VIC, Australia

*Corresponding Author: spalanisamy@swin.edu.au

Abstract: Titanium and its alloys have been used in a broad range of products such as biomedical implants due to their high specific strength, corrosion resistance and biocompatibility. Improvement in microstructure and mechanical properties of CP titanium is usually performed by cold rolling and controlled atmosphere heat treatment that is energy-intensive and costly. This study aims to investigate the effect of an in-situ electro-plastic treatment (ISEPT) on the microstructure evolution of commercially pure (CP) titanium. The deformation load and electric current in this treatment were applied in the same direction (in-situ) to maximise the electro-plastic effect. Simultaneous electric current and strain application created a condition for dynamic recrystallization to occur at low temperature and under atmospheric conditions, thus reducing the cost and energy for manufacturing. The rapid heating and cooling prevented the oxidation of titanium to a large degree, eliminating the costly inert gas or vacuum requirement. Results in relation to the effect of applied current, strain rate, cold working and geometry on the processed CP Ti were discussed.

Keywords:

Titanium, Resistant heating, Thermomechanical treatment, Electro-plastic deformation, Recrystallization, Grain refinement.

1. Introduction

Commercial purity (CP) titanium grades have exceptional properties of high strength-to-weight ratio, high corrosion resistance, and relatively high melting point [1]. CP-Ti is widely used in chemical processing and heat exchangers that deal with the severe corrosive environment and prosthetic parts in biomedical applications [2]. Titanium, however, is more expensive than the other rival light alloys and stainless steel partly due to the high cost of processing, such as vacuum or controlled atmosphere required during the remelting and heat treatment of ingot and downstream fabrication. The controlled atmosphere at high temperatures is necessary to prevent titanium from excessive reactivity with oxygen and hydrogen that causes embrittlement [1, 2]. Many research works have been published that suggest alternative cost-effective near net-shaped titanium parts or bulk titanium manufacturing routes, including hybrid and additive manufacturing [3, 4]. The hybrid processing method mainly involves powder sintering and post-consolidation treatments [5, 6], which inevitably requires a costly and energy-intensive controlled atmosphere.

The use of rapid heat treatment methods on titanium alloys has been studied for many years and showed exceptional ability in grain refinement and mechanical properties enhancement [7-10]. These processes include electric resistance heating, induction heating, or molten salt bath heating [7-10]. However, these works [7-10] focus mainly on annealed titanium (α-β) alloys and not on

CP-Ti grades that are known for their limited response to heat treatment alone due to their very low alloying elements content [1]. In addition, these published works involved the use of inert gas in their process. Electrically Assisted Forming (EAF) and electric-assisted manufacturing (EAM) have revealed exceptional ability to reduce the flow stress and increase material's formability [11, 12]. EAF involves the electric current application during deformation that results in the "electro-plastic effect". The electro-plastic effect is explained by three combined mechanisms of Joule heating, dislocations interaction, and metallic bond weakening that work together in reducing the deformation flow stress and increasing material's formability [11]. The EAF is best deployed on low formability alloys, especially titanium and magnesium alloys, with benefits to reducing deformation flow stress and spring back [11]. Xu & Chen [13] demonstrated that there is more than just Joule heating and softening effect when resistant heating was used for α-titanium deformation. The electric current was found to produce a higher heating rate to reach the final annealing temperature introducing complicated events in the EAF process. For example, the rapid heating rate caused by the momentum transfer from the electron drift into the crystal lattice improves the nucleation rate during recrystallization, which is explained by the "electron wind effect" [11, 13]. However, increasing the current density while maintaining the contact temperature of 600 °C resulted in grain growth caused by the increased grain boundaries migration rate explained by the electric current drift effect [11].

Salandro et al. [11] investigated the effect of electro-plastic kinetics when an electric current was applied through metals during deformation and compared it to conventional isothermal oven heating. First, it was observed that the Joule heating has different kinetics compared to isothermal heating, the former occurring by scattering electrons off interfacial defects (voids, impurities, grain boundaries) within the lattice, while the latter occurring by vibrational energy transfer via convection or radiation that results in uniform temperature distribution. Resistance heating is nonuniform, and it results in a higher temperature in the region surrounding the interfacial defects with higher energy. It is caused by electrons scattering, compared to other regions, although the gained vibrational energy will spread to the other regions forming temperature gradients. Second, direct dislocation-electron interaction assists dislocation motion in the case of electric resistance heating. Third, the electron flow plays an additional role in weakening the metallic bond, resulting in further softening and flow stress reduction [11].

The temperature profile in the electric-assisted compression test revealed a temperature drop during deformation, indicating the supplied power was partially consumed in assisting dislocation motion [11]. The electric-assisted deformation's stress-strain profile also showed a drop in flow stress and prolonged formability compared to the isothermal test with a similar temperature [11]. The resulting microstructure after titanium EAF tests consisted of equiaxed grains with variable grain size, a character of dynamic recrystallization caused by electric resistance heating. Salandro et al. [10] studied the temperature variation through the cross-section led to a change in heat input and straining that affected recrystallized grains nucleation rate and grain growth. Comparing the stress-strain profile of the EAF test to the schematic presentation of the flow curves for dynamic recovery and dynamic recrystallization, published by Zahiri et al. [14], also showed the similarity of the dynamic recrystallization curve with the presence of peak stress followed by a decrease in stress.

Titanium tendency to pick up oxygen generally initiates at approximately 550 °C [1]. Previous work by An et al. [15] revealed the ability to completely recrystallise cold-worked CP-Ti at 450 °C using non-isothermal warm rolling with a 90 °C temperature gap between the two rollers. This

indicated the possibility for recrystallization to occur at temperatures below the critical temperature for the oxidation of titanium (500-600 °C) [1], where the internal energy works as the driving force for dynamic recrystallization. In Humphrey et al. [16] work on recrystallization and annealing, the recrystallization temperature decreases as the thermomechanical process strain increases. A low heating rate encourages dynamic recovery reducing the required driving force for recrystallization [16].

This study aims to investigate the effect of an In-situ Electro-plastic Treatment (ISEPT) on commercially pure titanium (CP-Ti) recrystallization and grain refinement. This study was with the consideration of limited published work on the simultaneous application of electric resistance heating and straining to introduce dynamic recrystallization in CP titanium under atmospheric conditions. It was demonstrated that under certain conditions, ISEPT produces partial and fully recrystallized structures when applied current and deformation speed (strain rate) was varied. The effect of sample geometry on the formation of new grains by ISEPT was investigated.

2. Materials and methods:

2.1. In-situ Electro-plastic treatment:

The ISEPT process used in this study consisted of a machine that was developed at the Commonwealth Scientific and Industrial Research Organisation (CSIRO) under patent no WO2018232451 [17]. The schematic diagram in Fig. 1 shows machine's two rollers were connected to the AC power source. The specimen was fed to the machine between two rollers via lifting the top roller using a piston and interlocked back to connect the electric circuit through the specimen. The current was applied in the same direction as the applied force to simultaneously heat and deform the specimen.

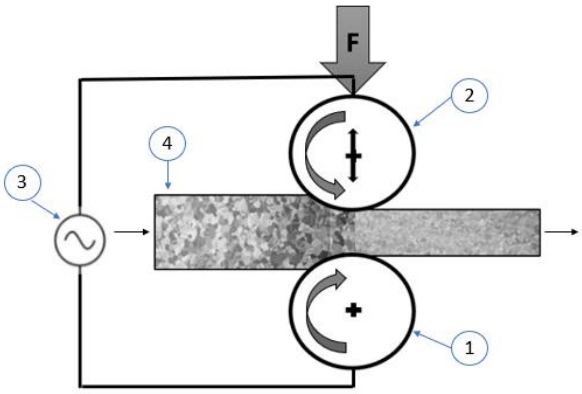

(a)

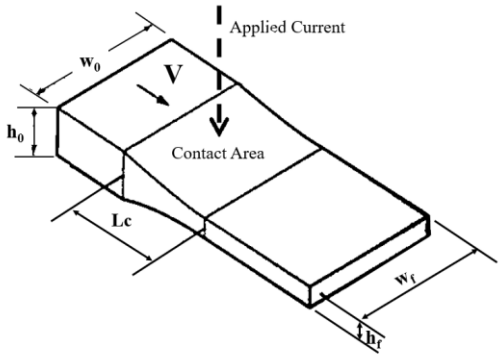

(b)

Fig. 1. (a) Schematic diagram of the in-situ electro-plastic treatment machine used in this study. (1) bottom roller (2) top roller (3) electric AC power source, (4) conductive specimen**, (b)** schematic of the sample geometry (rollers omitted) during the process and the applied current direction.

2.2. Materials used:

Three types of commercially pure titanium (CP-Ti) specimens were used to assess the effect of electro-plastic treatment on recrystallization with consideration of the sample (cross-section) geometry:

(a) CP-Ti Wire: Readymade annealed wire of 2.38 mm diameter.
(b) CP-Ti Strips: Two strips of machined rectangular cross-sections 6.5×5 mm and 5×3 mm.
(c) Cold worked CP-Ti Strip: Rectangular cross-section 3×5 mm and cold-rolled to 30% reduction in thickness.

The rectangular strips were machined from a CP-Ti grade-2 plate with composition and properties shown in Table 1.

Table 1 Properties and chemical composition of the CP-Ti strips.

Chemical composition (wt%)	
Titanium	Balance
Fe	0.3
C	0.08
N	0.03
H	0.015
O	0.25
Mechanical properties	
Tensile strength (MPa)	345
Yield Strength (MPa)	275-450
Elongation (%)	20
Density (g/cm^3)	4.7

The microstructure of the CP-Ti wire and CP-Ti strips were examined before and after the electro-plastic treatments. Samples were cut perpendicular to the rolling direction in all experiments, and cold mounted in epoxy moulds, grounded progressively down to 2000 grit using SiC papers for light microscopy. Overheating during grounding and cutting was avoided using a cooling medium. Progressive polishing down to 1 µm was used, followed by the final OP-S mix with ammonia and hydrogen peroxide etch-polishing.

The mechanical property of CP-Ti samples before and after electro-plastic treatment was measured by HV microhardness under 300-N load to quantify materials softening behaviour. LECO Inert gas Fusion Analyser Model-ONH836 series, by LECO Corporation, USA, was used to determine oxygen and nitrogen content before and after treatments. All electro-plastic experiments were conducted under atmospheric conditions in the absence of inert gas.

3. Results:

The main process parameters for the electro-plastic treatment of this study were the applied load, applied current and the rolling surface speed (RSS). The effect of these parameters on CP-Ti microstructure, grain size and microhardness were determined.

3.1. Electro-plastic treatment of CP-Ti wire

A stock of annealed CP-Ti wire of 2.38 mm diameter was used in the ISEP treatment. The applied 0.7 MPa pressure and 1.5 kA current were kept constant in all experiments, and the RSS was gradually increased from 0.52 mm/s (0.038 s^{-1} strain rate) to 19.5 mm/s (0.74 s^{-1}), as shown in Fig. 2. The results showed an increase in RSS led to the rise in the strain rate with a less achievable reduction in thickness. At the lowest RSS of 0.52 mm/s, the sample thickness reduced by 58.6%. This was equal to 0.88 true strain at a strain rate of 0.04 s^{-1} compared to the highest RSS of 19.5 mm/s, which resulted in a 0.3 true strain and 0.74 s^{-1}strain rate with a 26% reduction.

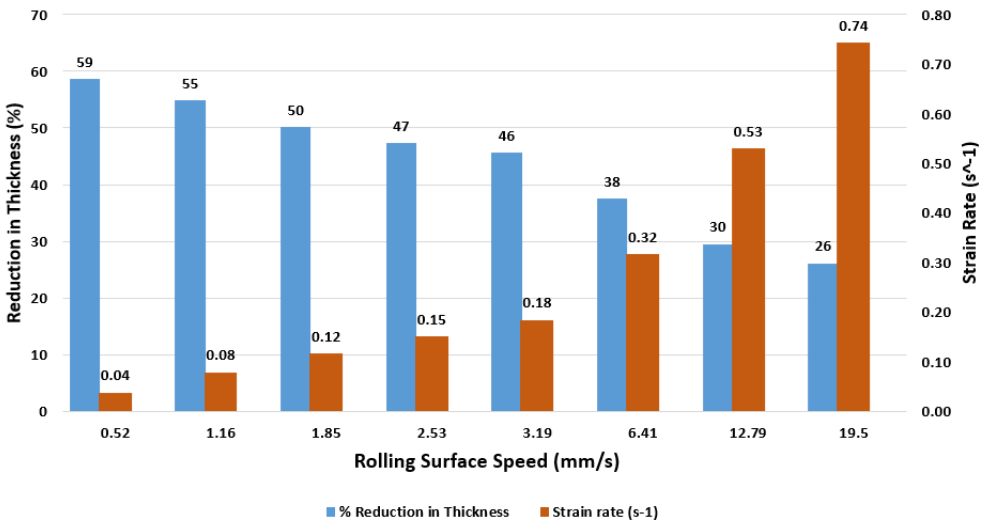

Fig. 2. The reduction (%) of sample thickness and strain rate as a function of electro-plastic rolling surface speed for CP Ti wire.

Fig. 3 revealed that, overall, an increase in rolling speed above 0.52 mm/s resulted in an improvement of hardness for conditions of this study. The hardness and grain size of the electro-plastically deformed materials were less than the original wire. Finer grains were created with an increasing strain rate up to RSS of 3.19 mm/s (0.18 s^{-1} strain rate), which was in agreement with the observations in the published literature [16]. However, a further increase in RSS (strain rate) above 3.19 mm/s retarded recrystallization with the formation of elongated grains was caused by a decrease in material exposure to the applied current. The samples showed insignificant change in oxygen and nitrogen content before and after ISEPT, as shown in Fig. 4. This is believed to result from the rapid heating rate and the lower recrystallization temperature associated with this treatment.

Fig. 5 shows a light microscope (LM) images of the CP-Ti wire cross-section before and after the treatment. The wire's initial microstructure had an average grain size of 25 µm, as seen in Fig. 5(a) and (b). Recrystallization and the X pattern of grain refinement were caused by strain variation along the cross-section, as shown in Fig.(5c,e, and g) that was in agreement with previous studies [18]. A minimum reduction of 35% was required to observe new dynamically recrystallized grains in the microstructure. Results in Fig. 3 and 5 suggested that an increase in RSS led to a reduction in dynamic recrystallization for conditions of this study. It is worth noting that for simplicity, we use the term 'dynamic recrystallization' to include meta-dynamic recrystallization [19, 20] as further study is required to differentiate these two processes under ISEPT conditions.

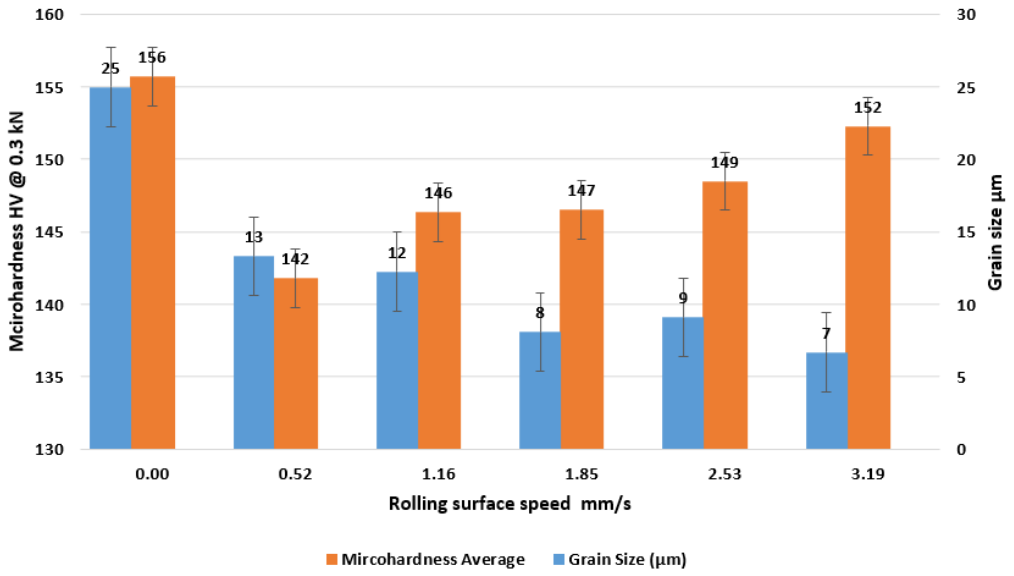

Fig. 3. Effect of rolling surface speed on grain size and microhardness of CP-Ti wire during ISEPT.

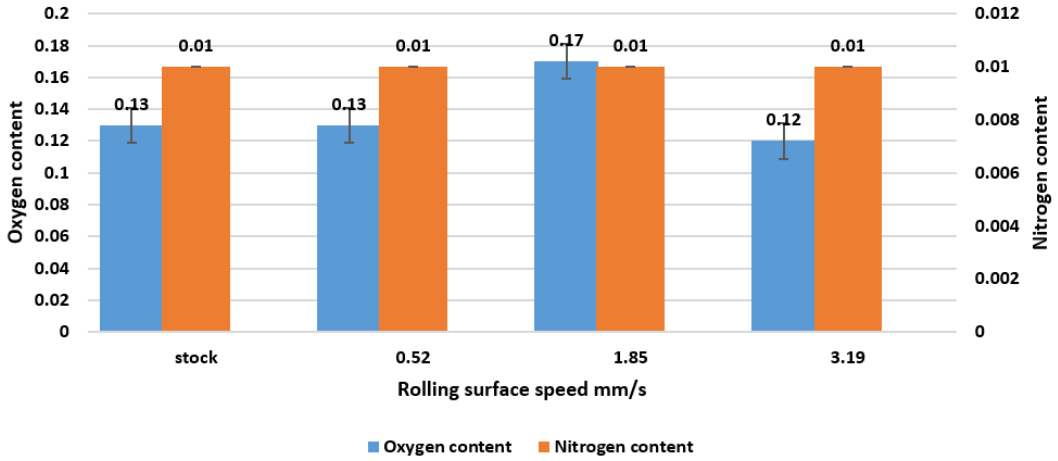

Fig. 4. Effect of rolling surface speed on oxygen and nitrogen content of CP-Ti wire during ISEPT.

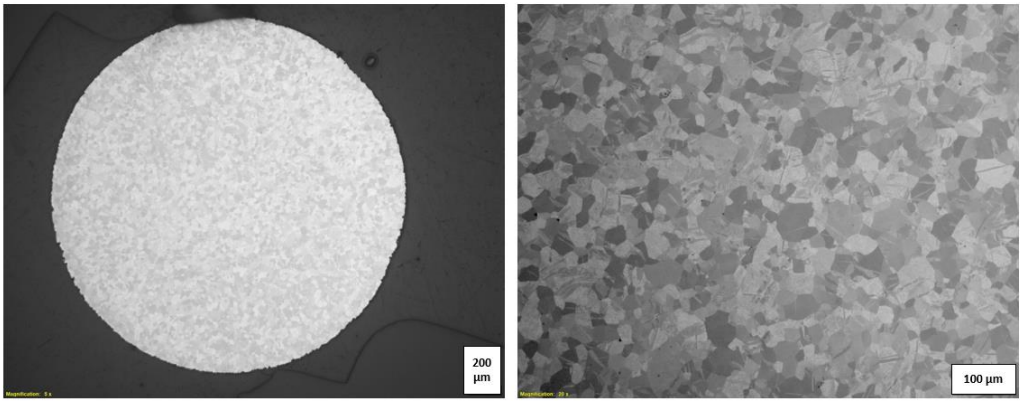

(a) (b)

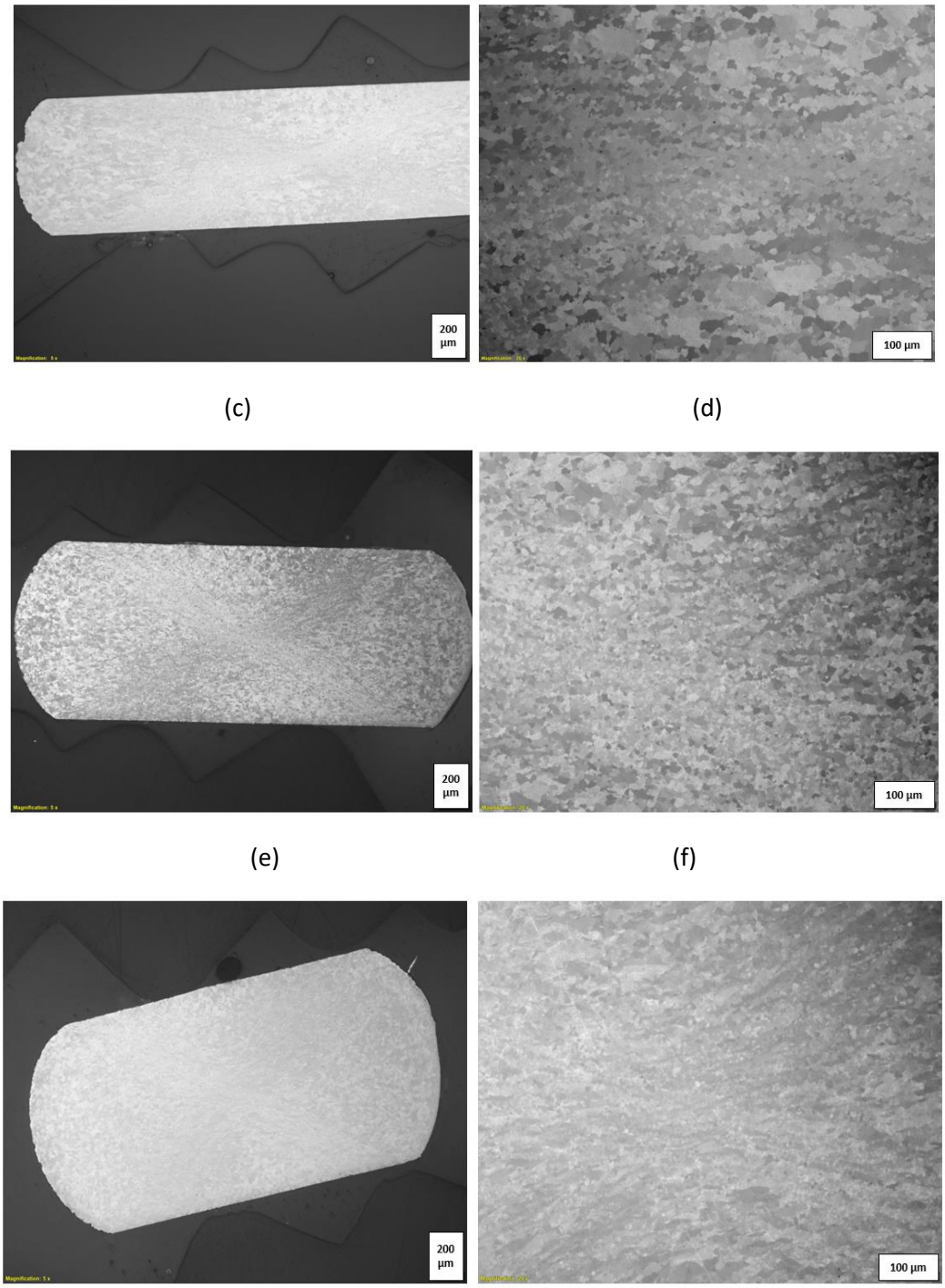

Fig. 5. LM microstructures of CP-Ti wire cross section, (a,b) before ISEPT, (c,d) at 0.52 mm/s (e,f) at 3.19 mm/s and (g,h) at 6.4 mm/s RSS.

3.2. Electro-plastic treatment of CP-Ti Strips

To determine the effect of sample geometry and size on ISEPT, CP Ti strips with 6.5×5 mm (32.5 mm^2) and 5×3 mm (15 mm^2) with rectangular cross-section were prepared, the cross-section

dimensions are w_0 and h_0 (Fig. 1(b)). The initial microstructure for the CP-Ti strip had an average grain size of 68 µm (Fig. 6).

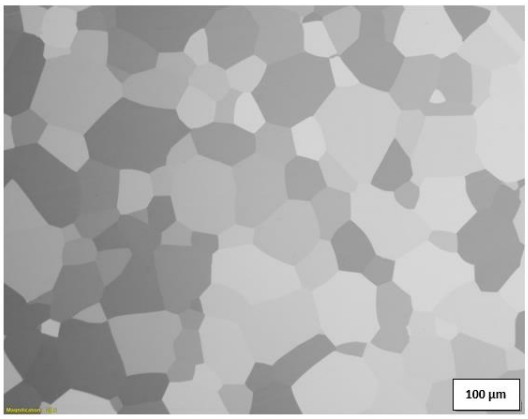

Fig. 6. LM image of CP-Ti strip initial microstructure.

The 6.5×5 mm CP-Ti strips were treated under similar processing conditions as the wire with a constant 1.5 kA current and 0.7 MPa pressure to compare the effect of RSS on (dynamic) recrystallization. As represented in Fig. 7, the results show a maximum 17.8% reduction in thickness at the lowest surface speed of 0.52 mm/s. Under this condition, a microstructure with grain boundary serration (Fig. 8(a)) was observed that resembled the first stage of dynamic recrystallization, as shown in Fig. 9 sourced from [16].

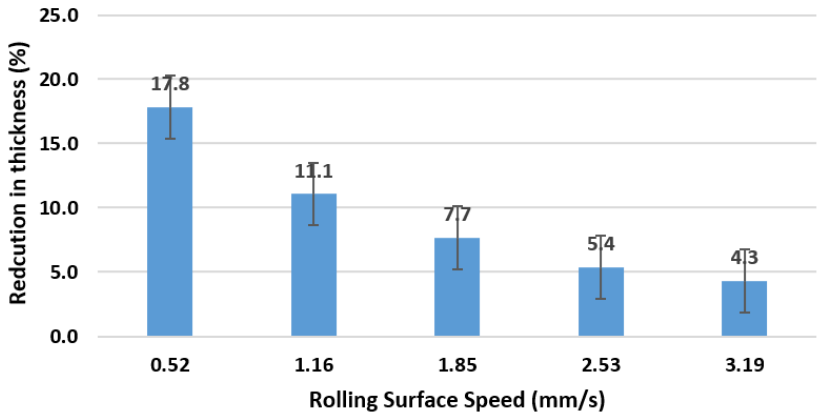

Fig. 7. RSS as a function of reduction for electro-plastic treated 6.5×5 mm CP-Ti strip.

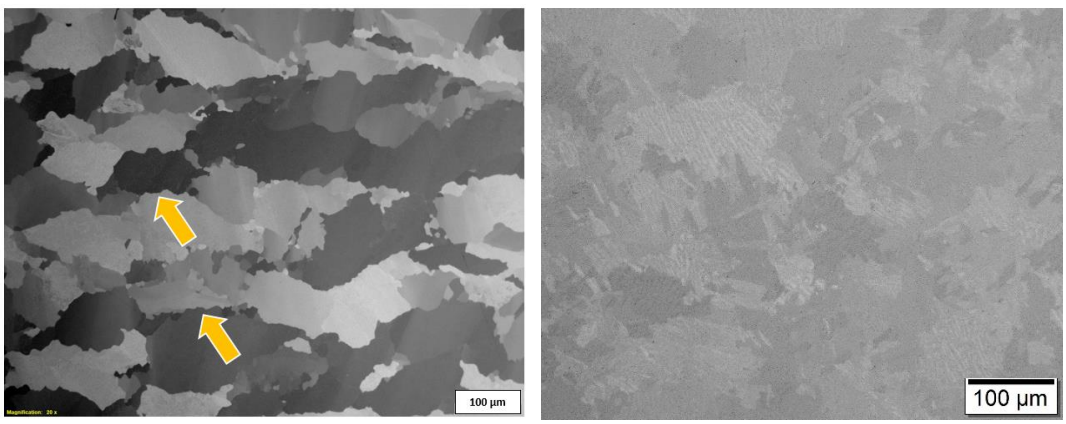

(a) **(b)**

Fig. 8. LM image of CP-Ti strip (a) at 0.52 mm/s RSS (arrows show grain boundary serration) and (b) at 1.16 mm/s RSS.

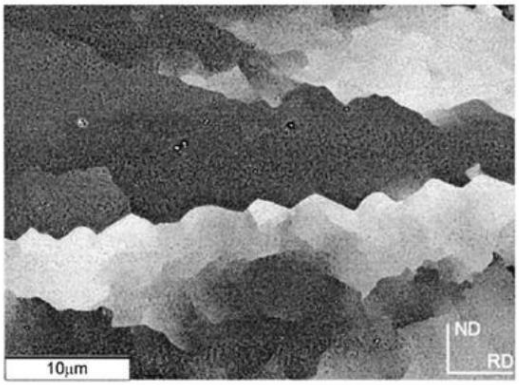

Fig. 9. Grain boundaries serration as reported by Humphreys et al. [16].

Recrystallized grains were not evident in other 6.5×5 mm (32.5 mm^2) samples when higher RSS than 0.52 mm/s was used. Insufficient (11%) reduction caused a lamellar microstructure with laths and twins at 1.16 mm/s surface speed, as shown in Fig. 8(b). Further increase in rolling speed contributed to a 7.7% reduction (Fig. 7) and less apparent microstructure changes.

3.3. Effect of strips cross-section:

To be able to study the effect of geometry on the CP Ti ISEPT, rectangular samples with a 5×3 mm cross-section that was ~50% less than previous 6.5×5 mm samples were deformed under two orientations. In the first orientation, the aspect ratio (AR), that is, the ratio of width to height of the strip, was considered to be <1. Therefore, w_0 in Fig. 1(b) was 3 mm, and h_0 was 5 mm when the 5x3 strip was deformed. The results showed an increase in the rollers' surface speed led to less deformation and straining of the samples (Fig. 10). The largest value for the reduction was ~34% at the lowest RSS of 0.52 mm/s. Under conditions of study, higher rolling speeds above 2.5 mm/s did not contribute to further reduction indicating the upper bound of rolling speed was reached.

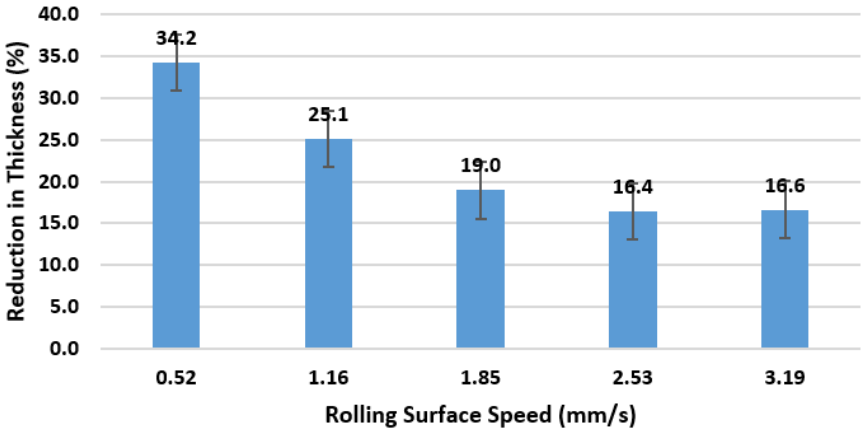

Fig. 10. Effect of RSS on thickness reduction for 5×3 mm cross-section CP Ti strip at 1.5 kA and 0.7 MPa.

The LM images corresponding to deformed samples in Fig. 10 are presented in Fig. 11. Compared with Fig. 6, partial recrystallization and necklacing were initiated at 0.52 mm/s and 1.16 mm/s rolling speeds, as shown in Fig.11(a) and (b), respectively. Further increase in rolling speed above 1.16 mm/s, Fig. 11(c-e), did not provide sufficient driving force for detectable recrystallization, mainly leading to the formation of twins and grain boundary serration.

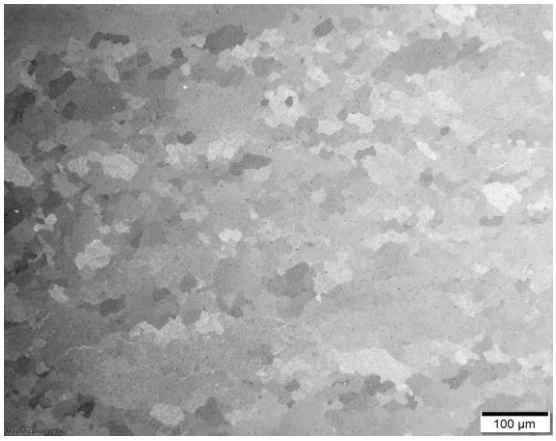

(a)

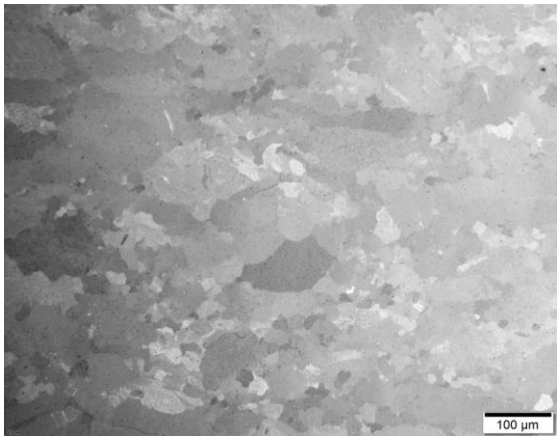

(b)

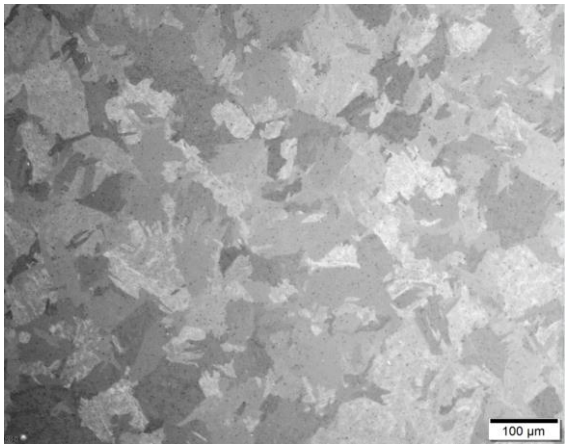

(c)

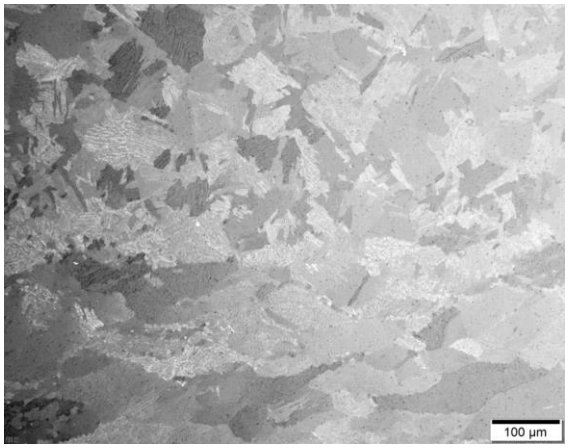

(d)

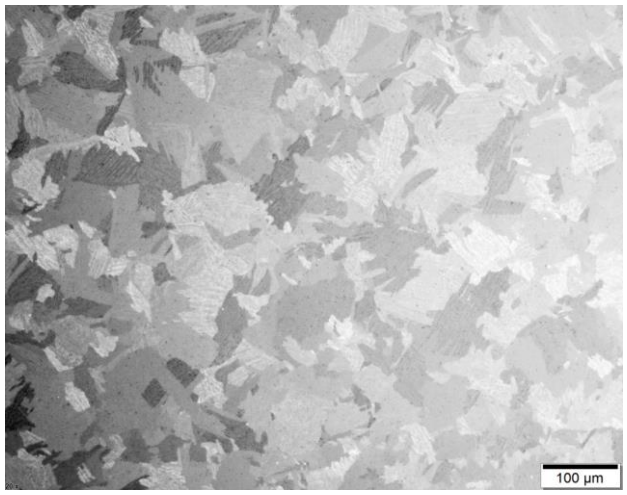

(e)

Fig. 11. Microstructure (LM) images of the electro-plastically deformed 3×5 mm CP-Ti strips at 1.5 kA and 0.7 MPa corresponding to (a) 0.52mm/s, (b) 1.16 mm/s, (c) 1.85 mm/s, (d) 2.53 mm/s and (e) 3.19 mm/s RSS.

The effect of the sample contact surface on the rollers under identical ISEPT conditions can be verified from Fig. 7 and 10. The sample with the smaller 3 mm width and AR <1 had the highest amount of deformation (34.2%). The contact surface difference between the 3 mm and 6.5 mm wide samples was at its maximum (~50%) when the lowest RSS was applied.

3.4. Effect of the applied current

Fig. 12 illustrated the influence of current on the electro-plastic deformation of 5×3 mm CP Ti strips when AR was <1. An increase in the applied current resulted in a higher reduction in thickness. The LM images related to Fig. 12 are shown in Fig. 11, Fig. 13, and Fig. 14. The results for the 2kA samples were mixed with the creation of refined recrystallized grains in some areas at 0.52 mm/s RSS and the formation of twins that became highly refined at the fastest 3.19 (mm/s) RSS (Fig. 13(a-e)). A similar trend in the evolution of microstructure was observed at 2.5 kA (Fig. 14(a-e)) that require further studies to determine the critical stress for the initiation of dynamic recrystallization.

Results in Fig. 12 suggest that at least 34% deformation was required to initiate recrystallization in CP Ti for conditions of this study. Overall, recrystallization at a lower current and slower surface speed (i.e. 1.5 kA and 0.52 mm/s) was more favourable for the initiation of dynamic recrystallization, as observed in Fig. 11, 13, and Fig. 14. Furthermore, the benefit of using less current in ISEPT manufacturing was to reduce energy consumption and to prevent excessive heating that could cause oxygen and nitrogen reaction with CP Ti under atmospheric conditions.

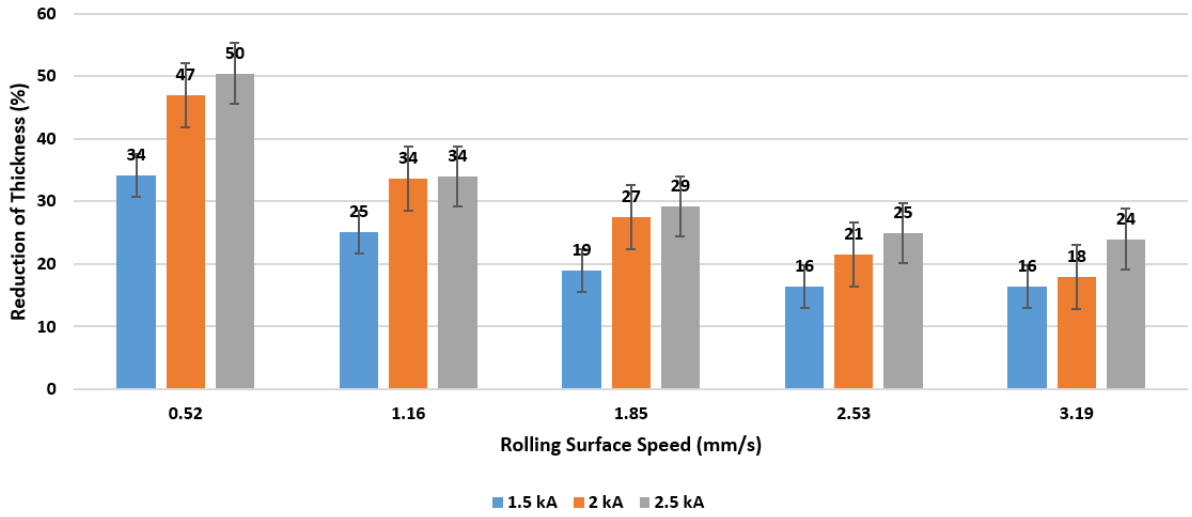

Fig. 12. Effect of the applied current on ISEPT of a 5×3 mm CP Ti strip at a constant 0.7 MPa rolling pressure.

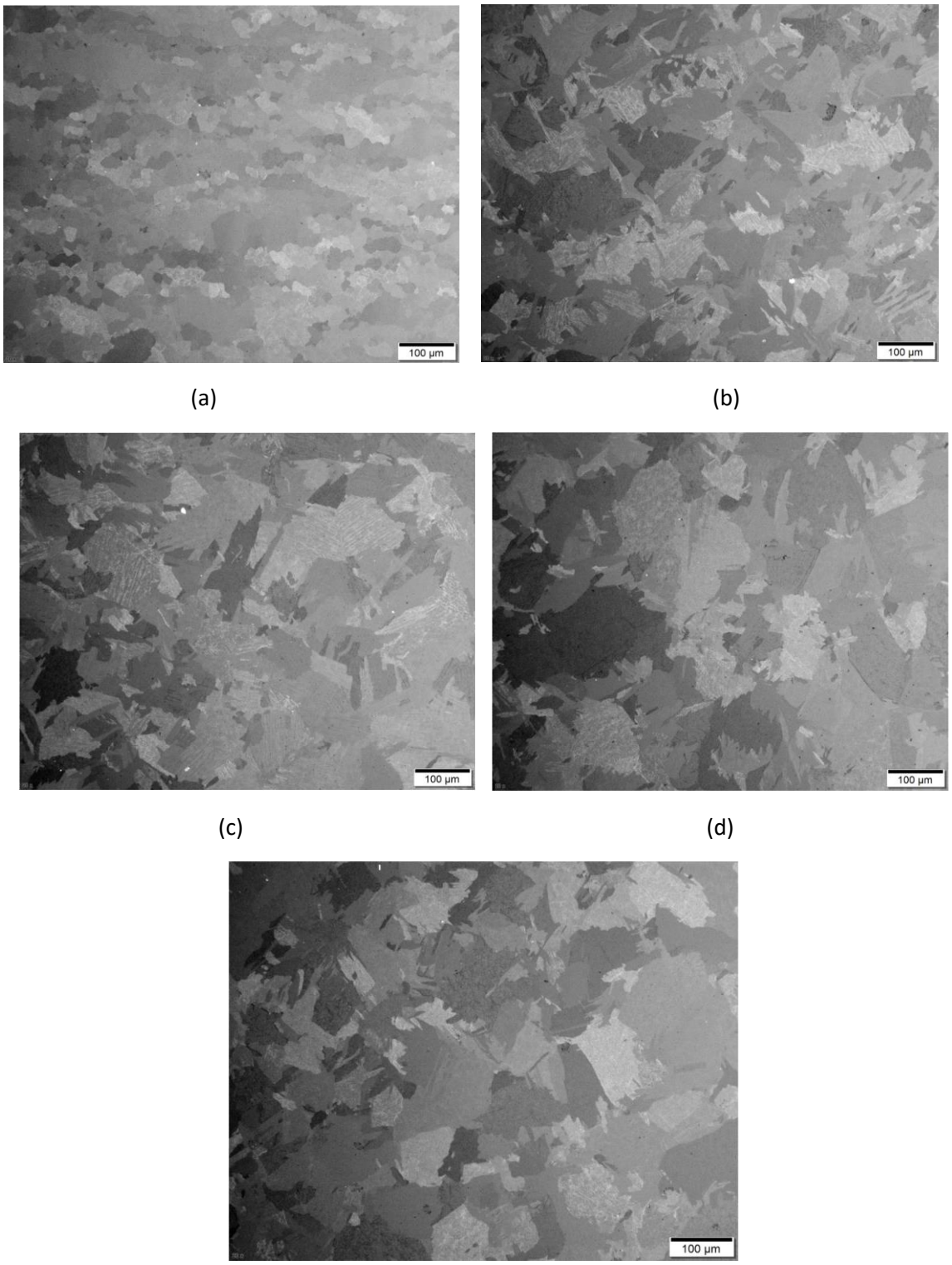

Fig. 13. LM images of 3×5 mm CP-Ti strip microstructure after ISEPT at 2.0 kA and 0.7 MPa corresponding to (a) 0.52mm/s, (b) 1.16 mm/s, (c) 1.85 mm/s, (d) 2.53 mm/s and (e) 3.19 mm/s RSS.

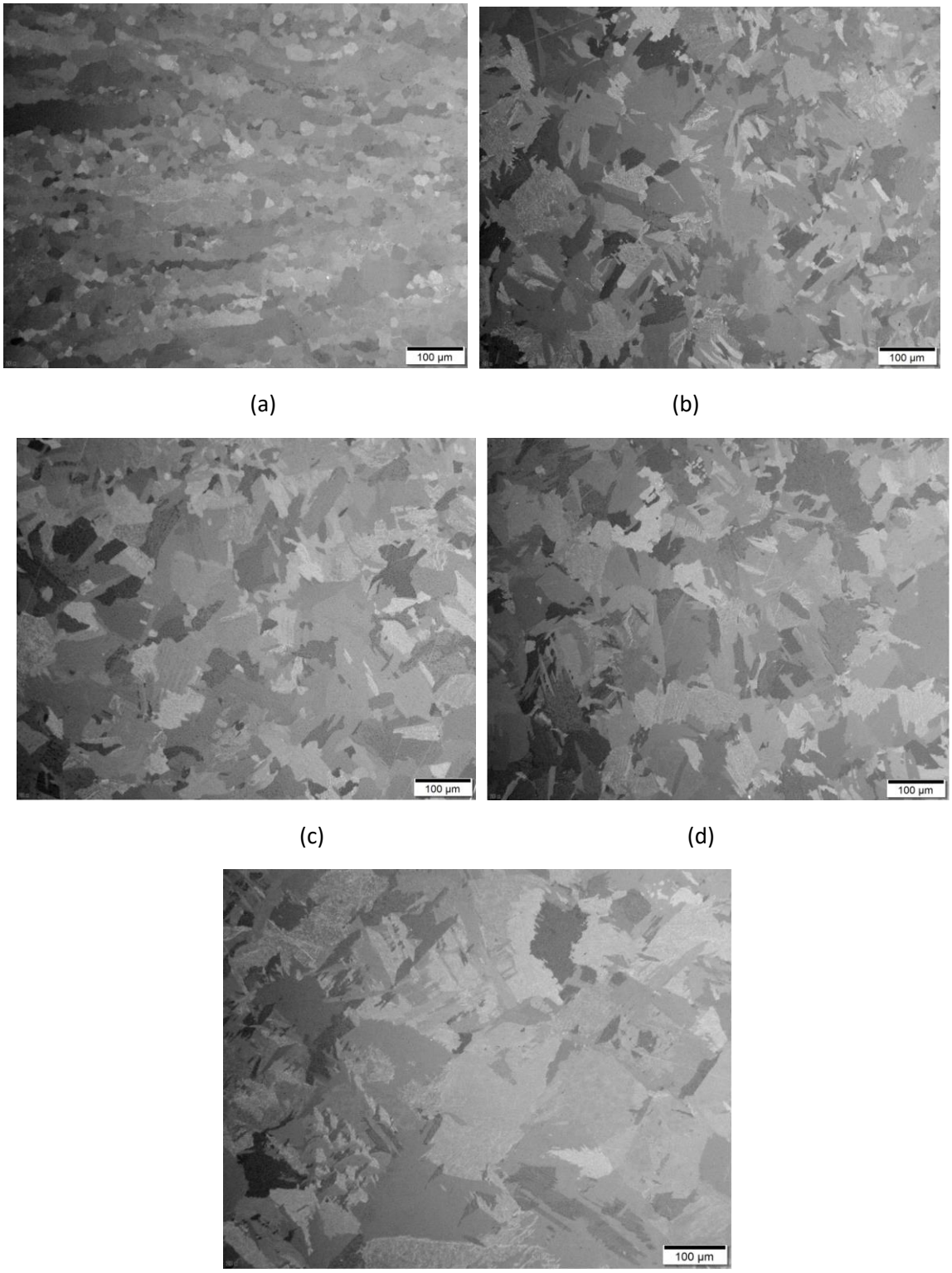

Fig. 14. LM images of 3×5 mm CP-Ti strip microstructure after ISEPT at 2.5 kA and 0.7 MPa corresponding to (a) 0.52mm/s, (b) 1.16 mm/s, (c) 1.85 mm/s, (d) 2.53 mm/s and (e) 3.19 mm/s RSS.

Qualitative comparison of the microstructures in Fig. 13(a) and 14(a) showed the appearance of more recrystallized grains when current increased from 2 to 2.5 kA. In agreement with an earlier study [11], a nonuniform mixture of large and small grains were observed at the highest applied

current (Fig. 14(a)). Fig. 11(c-e), 14(b-e) and 15(b-e) show further coarsening of a lamellar structure with twins in the absence of recrystallization; this could be explained by the retained heat in the samples at higher rolling speed. A similar event occurs in hot rolling processes that are caused by a short time of contact between rollers and material at high rolling speeds [21].

3.5. Effect of rolling orientation:

To study the effect of specimen rolling orientation on the in situ electro-plastic deformations, the 5×3 mm sample was rotated 90° and rolled in such a way that the 5 mm side of the sample faced the rollers surface denoted as "Horizontal orientation". This corresponded to w_0=5mm and initial roller gap h_0=3mm in Fig.1(b) with AR of the strip >1. This study was to compare the results with "Normal orientation" conditions when strip AR was <1. Compared with Normal orientation, a significant decrease in reduction from 34% to 18% was observed after horizontal deformation (Fig. 15). The electro-plastic treatment's sensitivity to the geometry and rolling orientation was further highlighted by the LM images in Fig. 16, which shows the absence of detectable recrystallized grains in horizontal specimens compared with recrystallized CP Ti in Fig. 11(a) and (b) in Normal orientation. This suggested that under identical conditions, ISEPT samples with AR<1 exhibit improved softening and recrystallization.

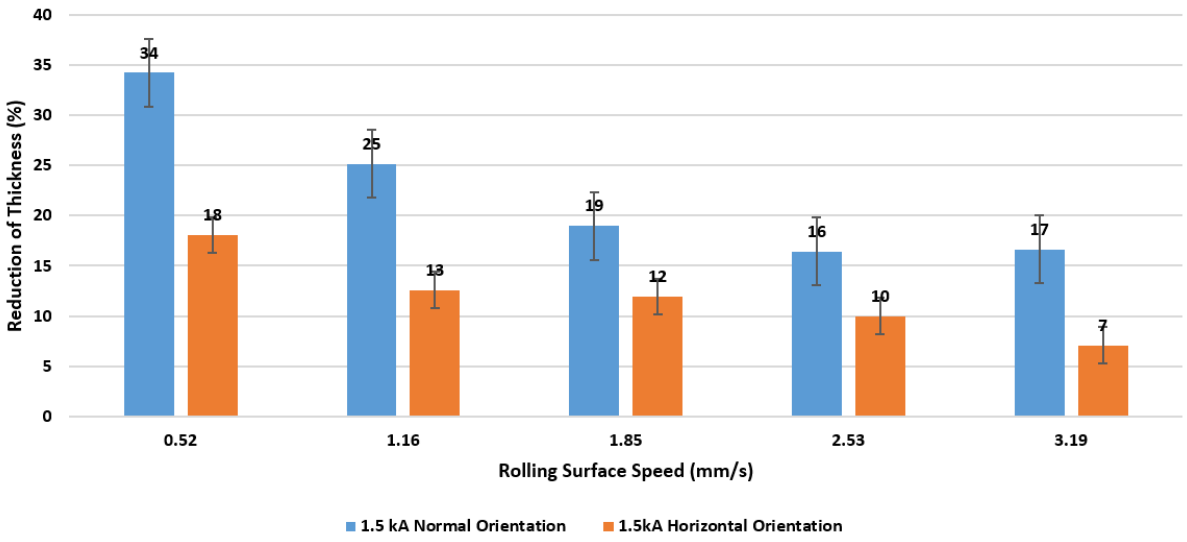

Fig. 15. Effect of electro-plastic rolling orientation on the reduction of 5x3 mm CP Ti strip.

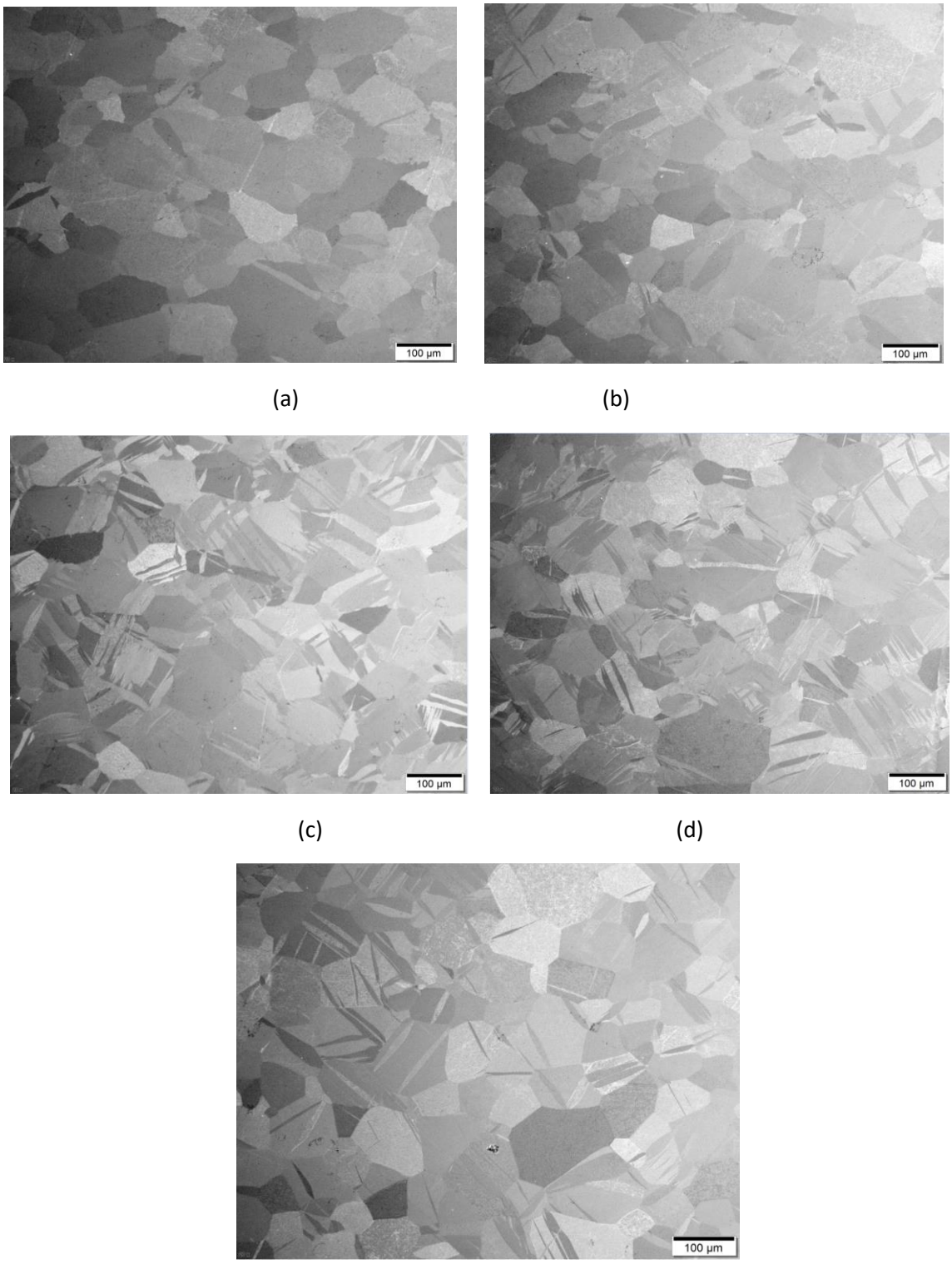

Fig. 16. LM images of ISEPT 5×3 mm CP Ti strips deformed under horizontal orientation at (a) 0.52 mm/s, (b) 1.16 mm/s, (c) 1.85 mm/s, (d) 2.53 mm/s and (e) 3.19 mm/s RSS.

3.6. Effect of cold working:

To examine the role of prior cold working on the effectiveness of the ISEPT, a CP Ti strip (5.25×3 mm cross-section) was cold-rolled in the Normal direction to 30% of its original thickness. The ISEPT conditions were 1.5 kA and 0.7 MPa load with similar RSS to previous experiments. Fig. 17

shows grain refinement was achieved at all RSS compared with experiments without cold working. Fig. 18 shows the pre-cold worked and electro-plastic treated microstructure at 0.52 mm/s surface speed resulted in a mainly uniform recrystallized microstructure with finer grain size than the original strip (Fig. 19(a) and 19(c)). Fig. 19(a-c) revealed the ISEPT microstructure evolution in agreement with the literature [16] on the impact of prior cold working on providing the required driving force for recrystallization. These qualitative results highlighted the contribution of electron flow interactions with dislocations and crystallographic defects in providing sufficient Joule heating and dislocation motion assistance to improve microstructural refinement [11].

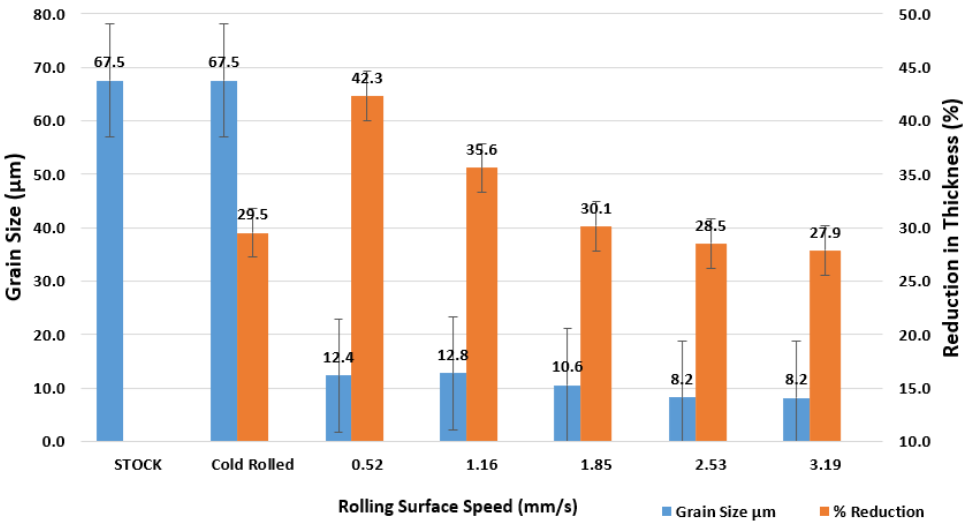

Fig. 17. Grain size and reduction as a function of RSS for 30% cold worked, and electro-plastic treated strip processed at 1.5 kA and 0.7 MPa.

Fig. 18. The low magnification microstructure (etched) of cold-worked and electro-plastic treated CP Ti strip at 1.5 kA, 0.7 MPa and 0.52 mm/s RSS, which is largely recrystallized.

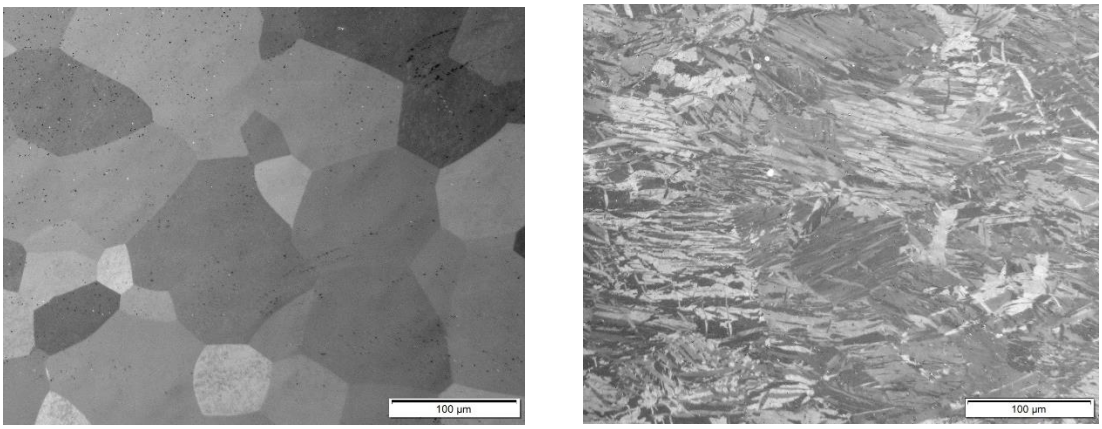

(a) (b)

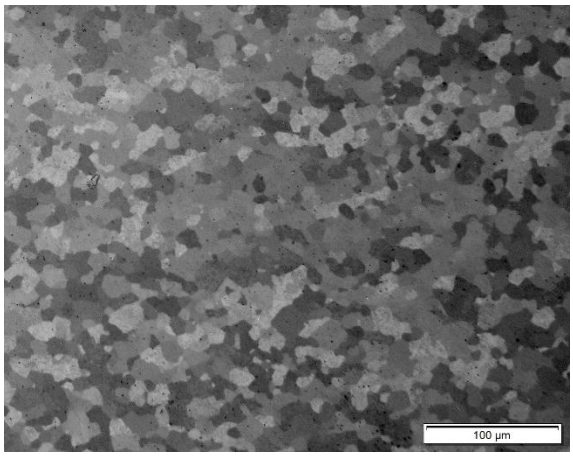

(C)

Fig. 19. LM images of CP Ti strip (a) as received microstructure, (b) the microstructure after 30% cold working, (c) recrystallized after ISEPT at 1.5 kA, 0.7 MPa, and 0.52 mm/s.

The microstructure of cold-rolled and electro-plastic treated specimens at different RSS is shown in Fig. 20 with corresponding grain size in Fig. 17. knowing that the initial grain size of the untreated strip was 67 µm, an increase in rolling speed resulted in marginal grain refinement. For example, Fig. 20(a) and Fig. 20(e) presented an average grain size of 12 µm and 8 µm, respectively. These results indicate the capability of the in-situ electro-plastic deformation to considerably refine CP Ti grain in a relatively short process time and without the need for inert gas or vacuum. Further to this, Fig. 20 and Fig. 17 confirm the ability of ISEPT to obtaining finer grains with increasing strain rate in agreement with the literature [16]. A potential benefit of this is to manufacture ultrafine grain structures (grain size <5 µm) [14] to improve further the mechanical properties of CP Ti that could be the subject of another study.

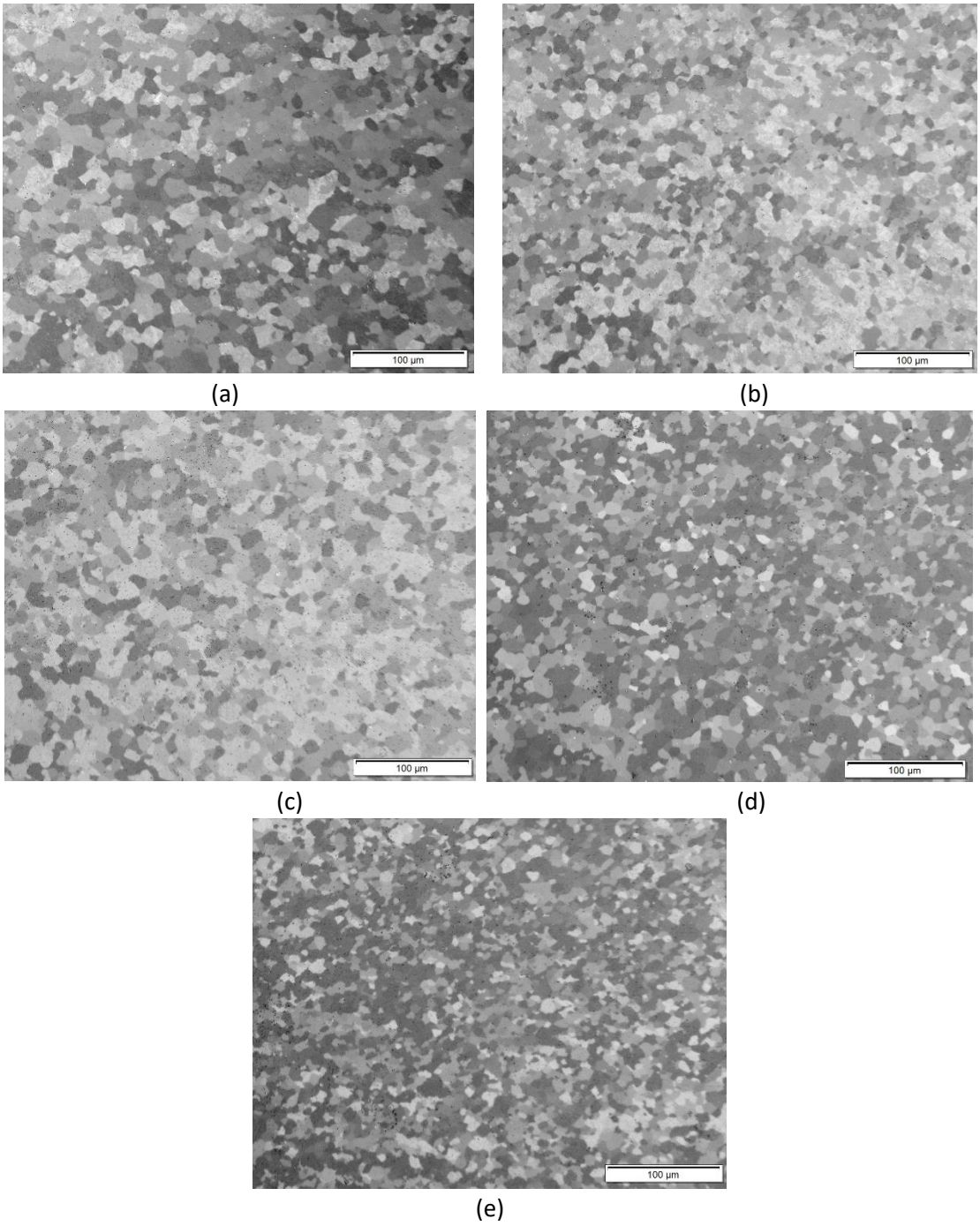

Fig. 20. LM images of CP Ti microstructure that was cold rolled prior to ISEPT at 1.5 kA, 0.7 MPa and, (a) 0.52 mm/s, (b) 1.16 mm/s, (c) 1.85 mm/s, (d) 2.53 mm/s, (e) 3.19 mm/s RSS.

4. Discussion:

Practical expressions that explain the relationship between the ISEPT parameters and developed microstructure generally consider the deformation variables such as the amount of reduction, strain, and strain rate in addition to current density and Joule heating.

Eq. (1) estimates the percentage of the reduction [22]:

$$r\% = \frac{h0-hf}{h0} \times 100 \quad (1)$$

Where $h0$, hf is the sample thickness before and after deformation, respectively (Fig. 1(b)).

The relationship between the applied strain and strain rate is expressed as Eq. (2).

$$\acute{\varepsilon} = \frac{RSS}{Lc}\ (\varepsilon) = \frac{RSS}{Lc}\ (ln\frac{h0}{hf}) \quad (2)$$

where ε is the true strain, έ is strain rate, RSS is the rollers rotational surface speed, and Lc is the contact length between the rollers and sample (Fig. 1(b)) estimated from Eq. (3)

$$Lc = \sqrt{r(h0 - hf)} \quad (3)$$

Where r is the roller's radius.

The rolling time (t) in Eq. (4) is derived from Eq. (2). The current application time (CAT) or heating time was considered similar to the rolling time for ISEPT due to the application of load and current under the same direction and simultaneously (Fig.1(b)).

$$t = \frac{Lc}{RSS} \quad (4)$$

The current density J was estimated using Eq. (5).

$$J = \frac{I}{A} \quad (5)$$

where I is the applied electric current, and A is the contact area (Lc × w_f in Fig. 1(b)), the area normal to the applied current direction. [11, 23]

Eq. (6) approximates the Joule heating energy

$$Q = I^2 R\ t \quad (6)$$

where I is the applied current, R is electrical resistance, and t is CAT estimated from Eq. (4) [23],

The samples resistance R in Eq. (6) is determined from the material's electrical resistivity and the sample dimensions (Fig. 1(b)) as Eq.(7):

$$R = \rho \frac{hf}{A} \quad (7)$$

where ρ is the material electrical resistivity (estimated for CP Ti = 0.000052 Ω-cm), h_f is the rollers gap in this study, and (A) the contact area (Lc × w_f) in Fig. 1(b).

4.1. Effect of Rolling Surface Speed (strain rate)

Fig. 21 and 22 show the estimated current density (Eq. (5)) and Joule heating (Eq.(6)) of the ISEPT in relation to applied RSS. The lowest RSS (0.52 mm/s) led to the lowest current density, and the highest Joule heating that coincided with the formation of CP Ti recrystallized grains (Fig. 11(a)). In contrast, high RSS, i.e. 3.19 mm/s (Fig. 21), caused the maximum current density and minimum Joule heating, resulting in excessive heating [21] from the short contact time and more effective roller chill.

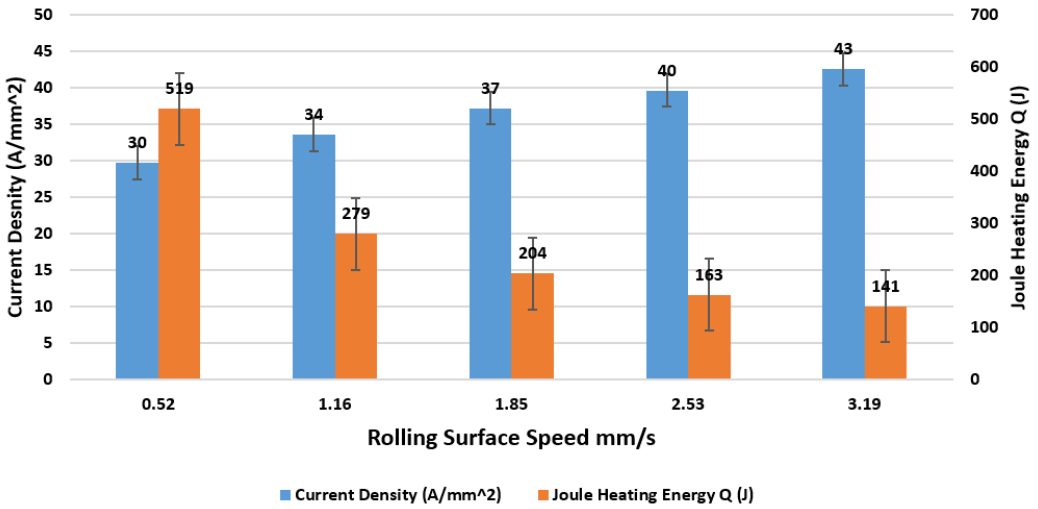

Fig. 21. The current density and Joule heating energy as a function of RSS for in-situ electro-plastic processed CP Ti wire at 1.5 kA and 0.7 MPa.

Eq. (7) shows a more pronounced effect of RSS at lower speeds on the CAT and reduced material resistance (Fig. 22) that raised the Joule heating energy in Fig. 21. The extended exposure of the sample at lower rolling speeds, i.e. 0.52 mm/s, was associated with the highest 22.86 seconds CAT that was related to the largest deformation (58%) in Fig. 2.

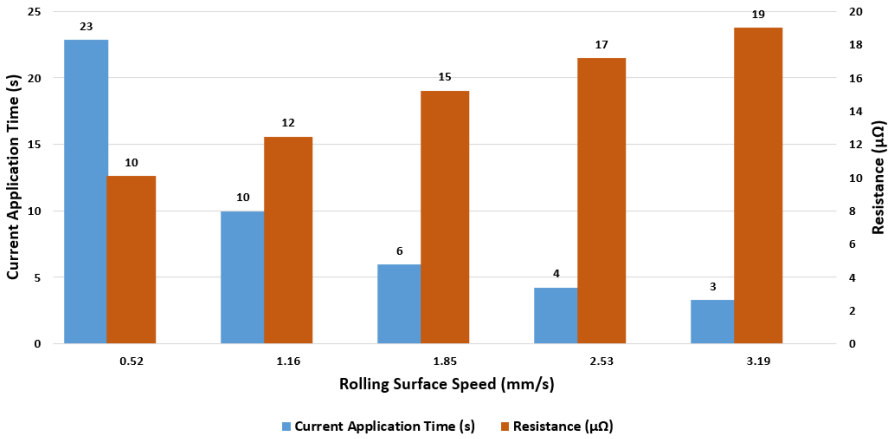

Fig. 22. The estimated sample's resistance (μΩ) and current application time (s) as a function of RSS for CP Ti Wire.

4.2. Effect of Sample Geometry and Aspect Ratio:

Fig. 23 shows the results for the effect of sample cross-section on current density and Joule heating. For example, at 0.52 (mm/s) RSS, the CP Ti wire, due to its circular and smaller cross-section, showed the highest value, 29.7 A/mm^2 (Fig. 24(a)). In contrast, the current density for 6.5×5 mm strip at 0.52 mm/s RSS was the lowest (21.9 A/mm^2) with increased contact area as expected. The highest current density at the fastest RSS (3.19 mm/s) had a limited effect on 6.5×5 mm strip deformation with the lowest 4.3% reduction in Fig. 7. This was the consequence of a considerable decrease in current application time and Joule heating, as shown in Fig. 23(b).

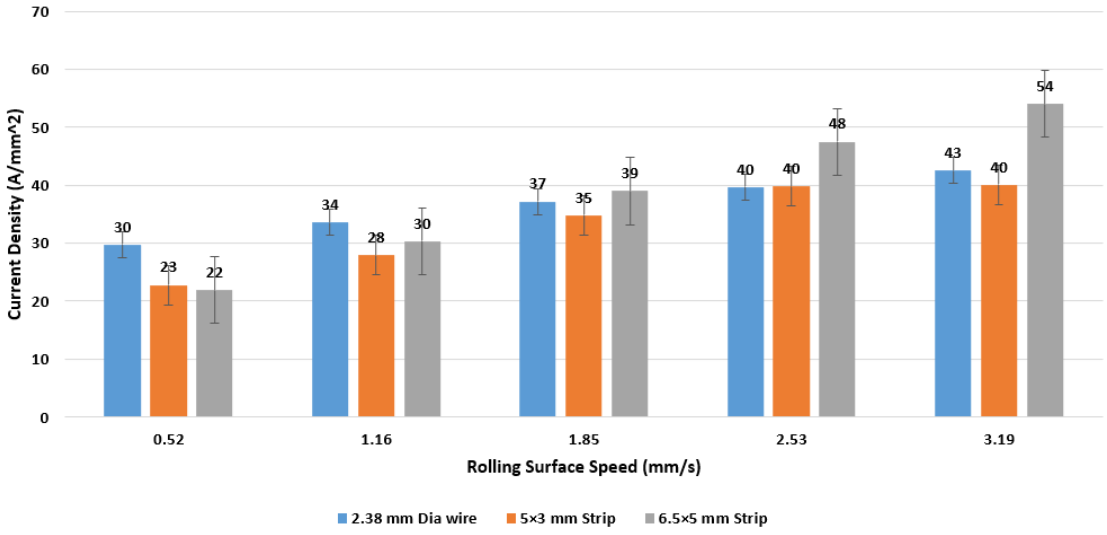

(a)

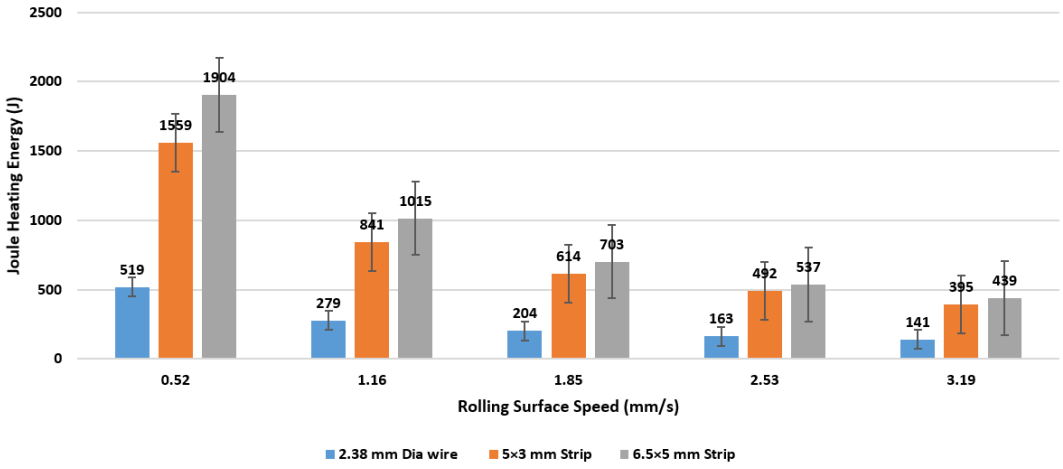

(b)

Fig. 23. Comparison of the CP Ti electro-plastic deformation for 2.38 mm diameter wire, 5×3 mm strip, and 6.5×5 mm strip as a function of RSS at 1.5kA and 0.7 MPa (a) current density (A/mm^2), and (b) Joule heating energy (J).

Fig. 23(b) shows that the estimated Joule heating energy from Eq. (6) increased with an increase in the sample's cross-section. In contrast to the wire with 58.6% reduction, the 6.5×5 mm strip with 1.9 kJ did not achieve sufficient straining (17.8% reduction) for recrystallization, as shown in Fig. 8(a). The consequence of this was mainly grain boundary serration. The 5×3 mm strip with 1.55 kJ and 22.8 A/mm^2 deformed 34 % with improved (partial) recrystallization, as seen in Fig. 11(a). It is worth noting that all conditions that allowed for some degree of softening prevented CP Ti under atmospheric conditions to react with oxygen and nitrogen, as shown in Fig. 4 chemical

analysis. In this regard, the ISEPT of CP Ti reduced the temperature and exposure time for the material to a level that the controlled atmosphere was unnecessary. Samples microstructure in Fig. 5,8,11,13, and 14 confirmed that excessive Joule heating does not improve the recrystallization outcome that was in agreement with the literature [11, 16].

The effect of strip aspect ratio (the ratio of w_f to h_f) on current density and Joule heating is presented in Fig. 24. An increase in RSS led to an increase in current density (Fig. 24(a)) with the opposite effect on Joule heating (Fig. 24(b)) that was consistent with earlier estimations for ISEPT of CP Ti wire. The most considerable reduction and recrystallization of the 5x3 mm strip were observed (Fig. 14(a)) when a combination of the lowest current density and the highest Joule heating achieved for the AR<1. These outcomes could be utilised to optimise ISEPT in relation to saving energy for the manufacture of CP Ti mill products.

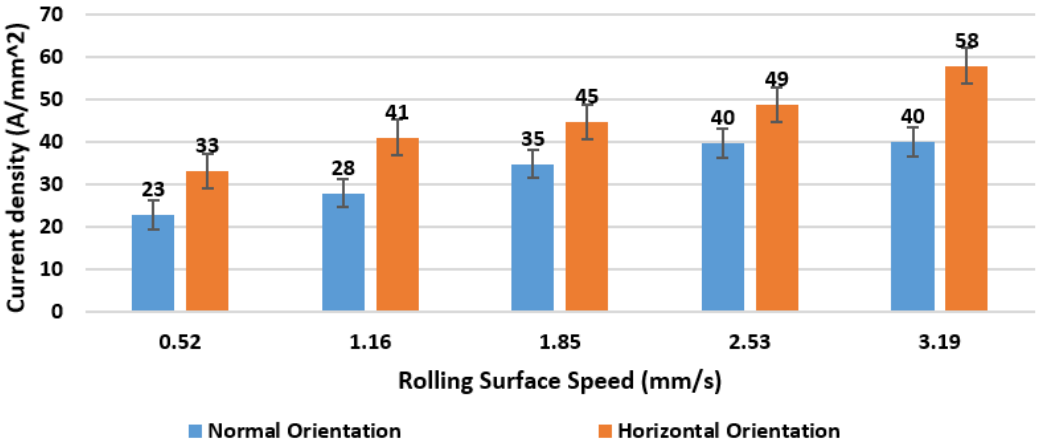

(a)

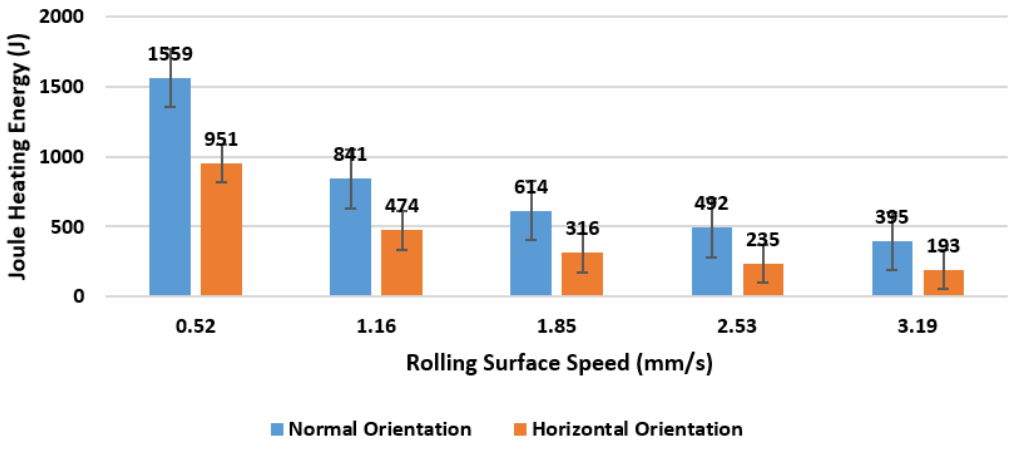

(b)

Fig. 24. Current density (a) and Joule heating energy (b) as a function of RSS for the 5×3 cross-section CP Ti strips rolled in horizontal and vertical orientations.

A more detailed analysis of the ISEPT parameters for the 5x3 strip at RSS 0.52 mm/s is shown in Fig. 25. The highest (34%) reduction was achieved when the sample had a normal orientation (AR<1). The resistance of the two samples had only a 10% difference. In contrast, CAT was 26s, almost double under normal rolling direction due to the larger contact length. The horizontal (AR>1) rolling resulted in greater current density but much lower Joule heating energy values, and the latter believed to be the reason for the low softening effect and reduced straining. The LM images of the horizontal rolling shown in Fig. 16 revealed the absence of recrystallization and grain refinement because of the limited 18% deformation. Result revealed an increase in current density without optimisation of Joule heating energy has a limited effect on the initiation of recrystallization.

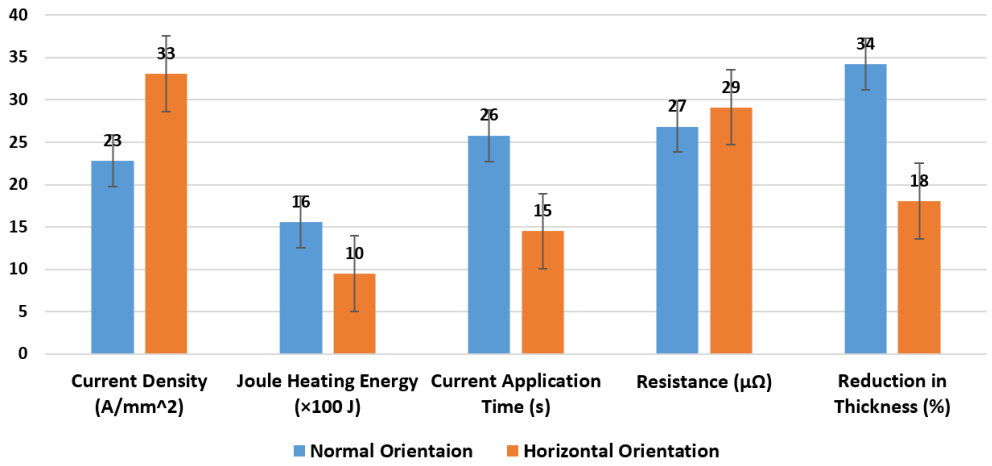

Fig. 25. Comparison of the parameters for horizontal and Normal electro-plastic treated 5×3 mm CP Ti strips at 1.5 kA, 0.7 MPa and 0.52 mm/s RSS.

4.3. Effect of Pre-Cold Rolling:

Recrystallized microstructures in relation to all RSS were only achieved when the CP Ti strip was cold-rolled prior to the ISEPT (Fig. 20). The effect of pre-cold work was to introduce dislocations that act as obstacles to the electron drift through the materials [11]. Furthermore, a higher number of dislocations in the material increased nucleation sites for new grains [16]. Another benefit of the dislocations that differentiated the current electro-plastic treatment with, i.e. warm rolling, was the interaction of the electric current (electrons) with the high-density dislocations that have been suggested to accelerate recrystallization [11]. Further studies that include measurement of the changes in CP Ti resistivity via cold working will be beneficial to understand its effect on ISEPT parameters.

A comparison of the normalised Joule heating energy for all samples in Fig. 26 allowed for comparison of the results in relation to applied RSS. Results for the pre-cold worked samples were not included due to insufficient information about the changes in resistivity of the CP Ti under deformation conditions of this study. The 2.38 mm Dia wire and the 5×3 Normal rolling orientation samples had matching plots at RSS 0.52 mm/s and 1.16 mm/s with 30 to 42 A/mm^2 current density. The smallest values for normalised Joules heating were for the 5×3 mm horizontal rolling orientation highlighted the importance of sample contact area on the ISEPT effectiveness for recrystallization.

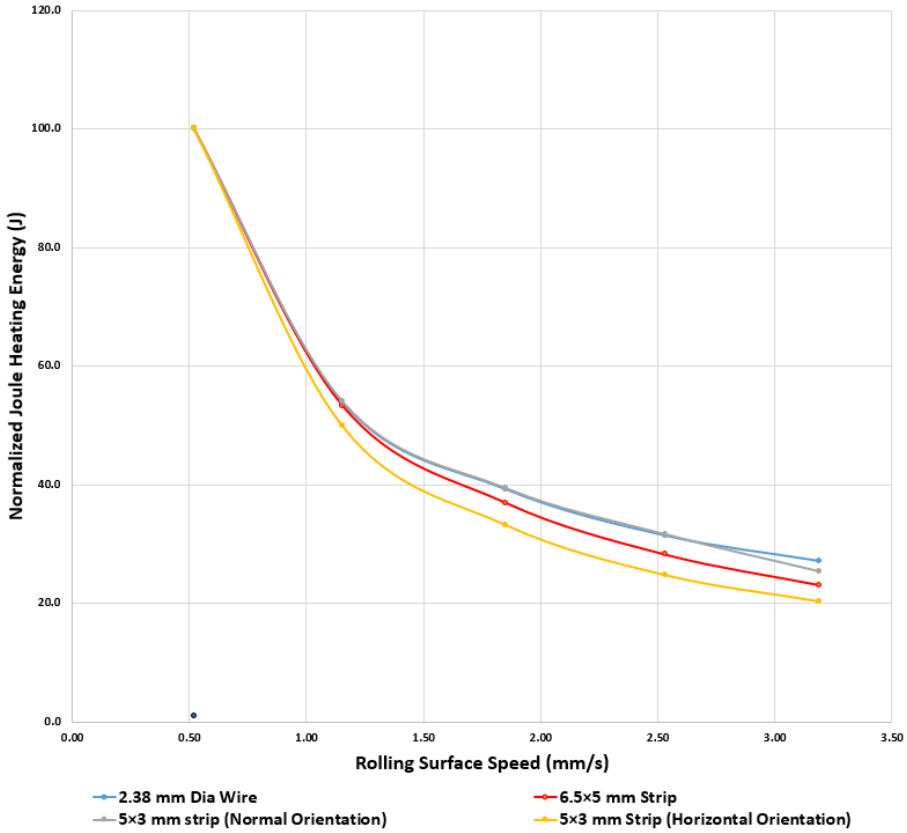

Fig. 26. Normalized Joule heating energy for the ISEPT samples.

5. **Conclusions**:

The effect of key process parameters of an in-situ electro-plastic treatment on microstructure, grain size and microhardness of an annealed and cold-worked CP-Ti were investigated. The ISEPT of CP Ti was conducted in air and without controlled atmosphere. The undetectable variations in oxygen and nitrogen content before and after the ISEPT suggested that recrystallization temperature was lower than the temperature for the oxidation of titanium. In this study, the process parameters were found to be highly dependent on the initial microstructure of the material. Introduction of higher dislocation density sourced from cold deformation improved recrystallization most likely due to the interaction of the material with the electrons flow.

The optimum ISEPT parameters to initiate formation of new grains were quantified as a minimum of 35% deformation with a maximum 3.19 mm/s surface speed at 1.5 kA equivalent to 42 A/mm^2 current density. The rolling surface speed (strain rate) affected current density, Joule heating energy, and specimen's achievable deformation.

It was found that the ISEPT led to improved recrystallization when the specimen rolling aspect ratio was <1. The rapid nature and low energy consumption of the ISEPT seem to be advantageous in relation to the conventional thermomechanical treatments to produce titanium mill products allowing utilisation of this material in broader engineering applications.

Ethical Approval: There is no requirements for ethical approval for this project.

Consent to Participate/Publish: All the authors consent to participate and contributed towards this work and publication in IJAMT journal.

Authors Contributions: Mohammed Abdul Khalik (MAK) – Contributed towards carrying out the research work writing the manuscript, Saden H. Zahiri: Concept development and initial experimental work and contribution towards manuscript , Syed H. Masood: Primary supervisor of this project, working with MAK, and contribution towards manuscript, Suresh Palanisamy: co-supervisor of MAK, contribution towards materials characterisation and writing of the manuscript and Stefan Gulizia: initial study and writing of the manuscript

Funding: This project is funded the Commonwealth Scientific and Industrial Research Organisation (CSIRO) and Swinburne University of Technology, Victoria, Australia.

Conflicts of interest/Competing interests: The authors declare that they have no known competing financial interests or personal relationships that could have appeared to influence the work reported in this paper.

Availability of data and material: The raw/processed data and materials required to reproduce these findings cannot be shared at this time as the data also forms part of an ongoing study.

References:

1. Lütjering, G. and J.C. Williams, *Titanium*. 2007: Springer Science & Business Media.
2. Leyens, C. and M. Peters, *Titanium and titanium alloys: fundamentals and applications*. 2003: John Wiley & Sons.
3. Childerhouse, T. and M. Jackson, *Near Net Shape Manufacture of Titanium Alloy Components from Powder and Wire: A Review of State-of-the-Art Process Routes.* Metals, 2019. **9**(6): p. 689.
4. Caiazzo, F., *Additive manufacturing by means of laser-aided directed metal deposition of titanium wire.* The International Journal of Advanced Manufacturing Technology, 2018. **96**(5): p. 2699-2707.
5. Weston, N.S. and M. Jackson, *FAST-forge– A new cost-effective hybrid processing route for consolidating titanium powder into near net shape forged components.* Journal of Materials Processing Technology, 2017. **243**: p. 335-346.
6. Doblin, C., G.M. Cantin, and S. Gulizia. *Processing TiROTM powder for strip production and other powder consolidation applications*. 2016. Trans Tech Publications Ltd.
7. Ivasishin, O.M. and P.E. Markovsky, *Enhancing the mechanical properties of titanium alloys with rapid heat treatment.* Jom, 1996. **48**(7): p. 48-52.
8. Ivasishin, O.M., *High strength microstructural forms developed in titanium alloys by rapid heat treatment.* Le Journal de Physique IV, 2001. **11**(PR4): p. Pr4-233-Pr4-240.
9. Ivasyshyn, O., P.E. Markovs'kyi, and I. Havrysh, *Formation of the Microstructure and Mechanical Properties of VT22 Titanium Alloy Under Nonequilibrium Conditions of Rapid Heat Treatment.* Materials Science, 2015. **51**(2): p. 158-164.
10. Ivasishin, O.M. and R.V. Teliovich, *Potential of rapid heat treatment of titanium alloys and steels.* Materials Science and Engineering: A, 1999. **263**(2): p. 142-154.
11. Salandro, W.A., et al., *Electrically assisted forming: Modeling and control*. 2014: Springer.
12. Ao, D., et al., *Experimental investigation on the deformation behaviors of Ti-6Al-4V sheet in electropulsing-assisted incremental forming.* The International Journal of Advanced Manufacturing Technology, 2019. **104**(9): p. 4243-4254.

13. Xu, Z.S. and Y.X. Chen, *Effect of electric current on the recrystallization behavior of cold worked α-Ti.* Scripta Metallurgica, 1988. **22**(2): p. 187-190.
14. Zahiri, S.H., C.H.J. Davies, and P.D. Hodgson, *A mechanical approach to quantify dynamic recrystallization in polycrystalline metals.* Scripta materialia, 2005. **52**(4): p. 299-304.
15. An, X.-z., X.-h. Rao, and Y.-n. Li, *Impact of non-isothermal warm rolling on microstructure, texture and mechanical properties.* ASME 2017 12th International Manufacturing Science and Engineering Conference collocated with the JSME/ASME 2017 6th International Conference on Materials and Processing: Volume 1: Processes, 2017.
16. Humphreys, F.J. and M. Hatherly, *Recrystallization and related annealing phenomena*. 2012: Elsevier.
17. Zahiri, S.H. and S. Gulizia, *Process for forming wrought structures using cold spray*, in *World international property organization*, WIPO, Editor. 2018.
18. Pope, J. and M. Jackson, *FAST-forge of Diffusion Bonded Dissimilar Titanium Alloys: A Novel Hybrid Processing Approach for Next Generation Near-Net Shape Components.* Metals, 2019. **9**(6): p. 654.
19. Zahiri, S.H., et al., *Models for Static and Metadynamic Recrystallisation of Interstitial Free Steels.* Materials science forum., 2005. **475**: p. 157-160.
20. Sakai, T., et al., *Dynamic and post-dynamic recrystallization under hot, cold and severe plastic deformation conditions.* Progress in materials science, 2014. **60**: p. 130-207.
21. Murthy, P.L.S., H. Patil, and B.N. Sarada, *Studies on influence of roller diameter and roller speed on process parameters in hot rolling process using manufacturing simulation.* Technical research organization India, 2016. **3**(5): p. 24-27.
22. Groover, M.P., *Fundamentals of modern manufacturing: materials, processes, and systems*. 2020: John Wiley & Sons.
23. Lupi, S., M. Forzan, and A. Aliferov, *Induction and direct resistance heating.* Switzerland: Springer, 2015.

Figures

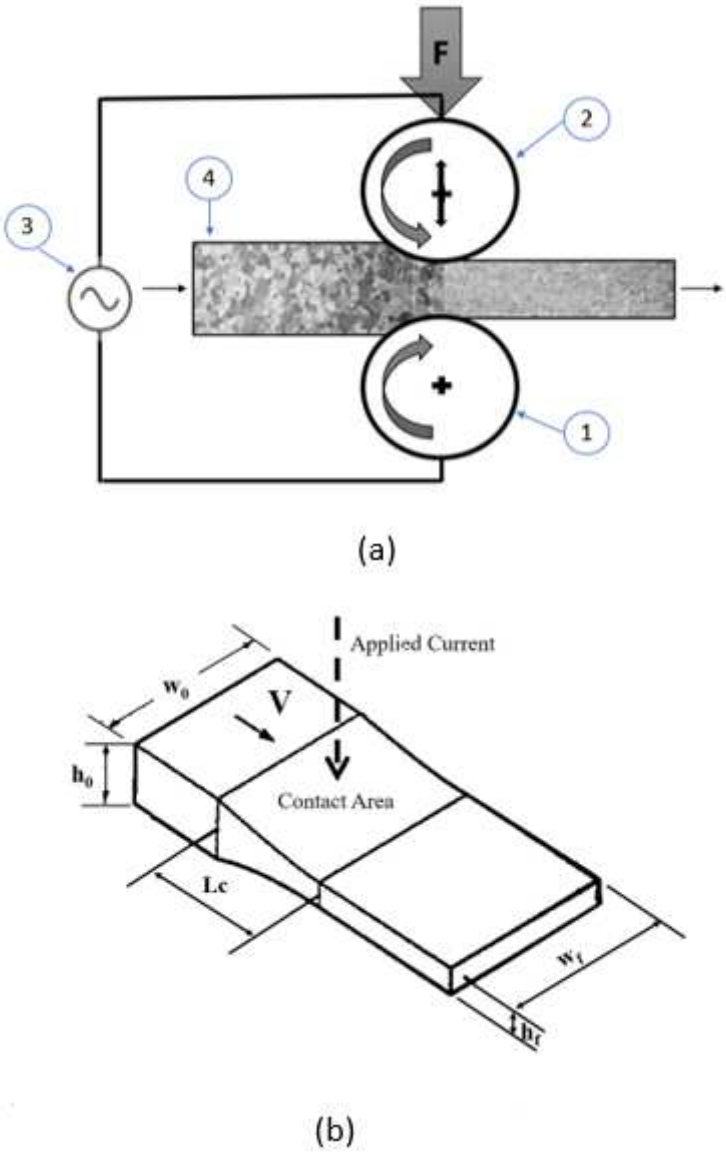

Figure 1

a) Schematic diagram of the in-situ electro-plastic treatment machine used in this study. (1) bottom roller (2) top roller (3) electric AC power source, (4) conductive specimen, (b) schematic of the sample geometry (rollers omitted) during the process and the applied current direction.

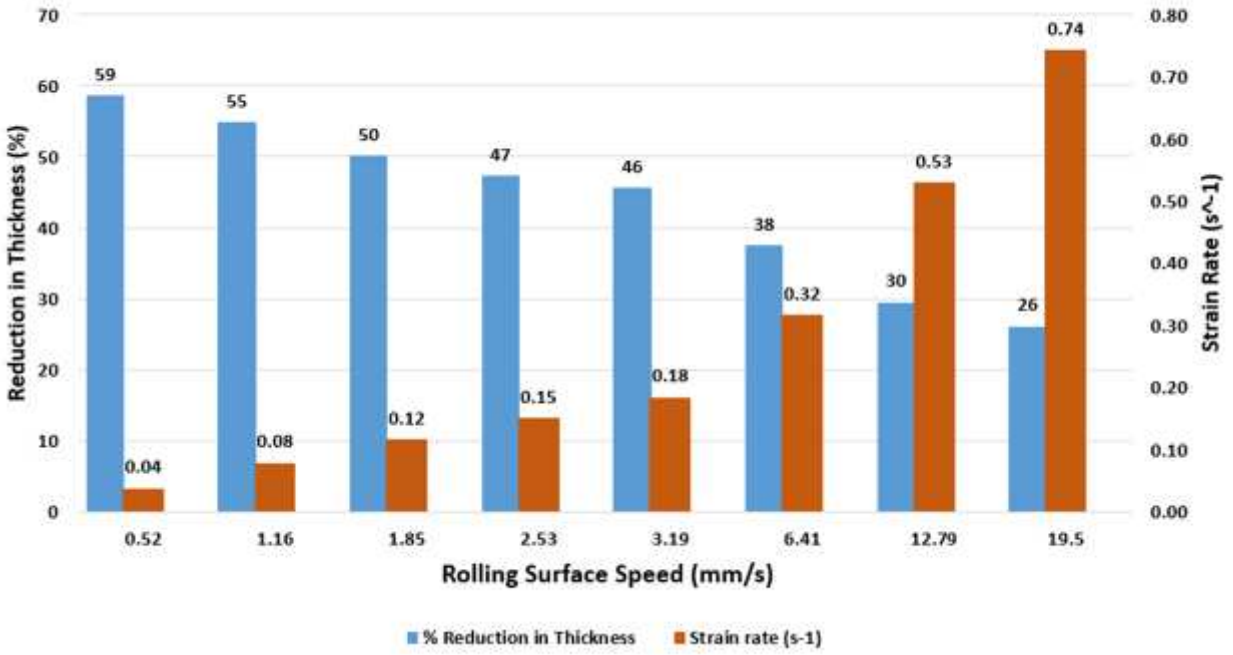

Figure 2

The reduction (%) of sample thickness and strain rate as a function of electro-plastic rolling surface speed for CP Ti wire.

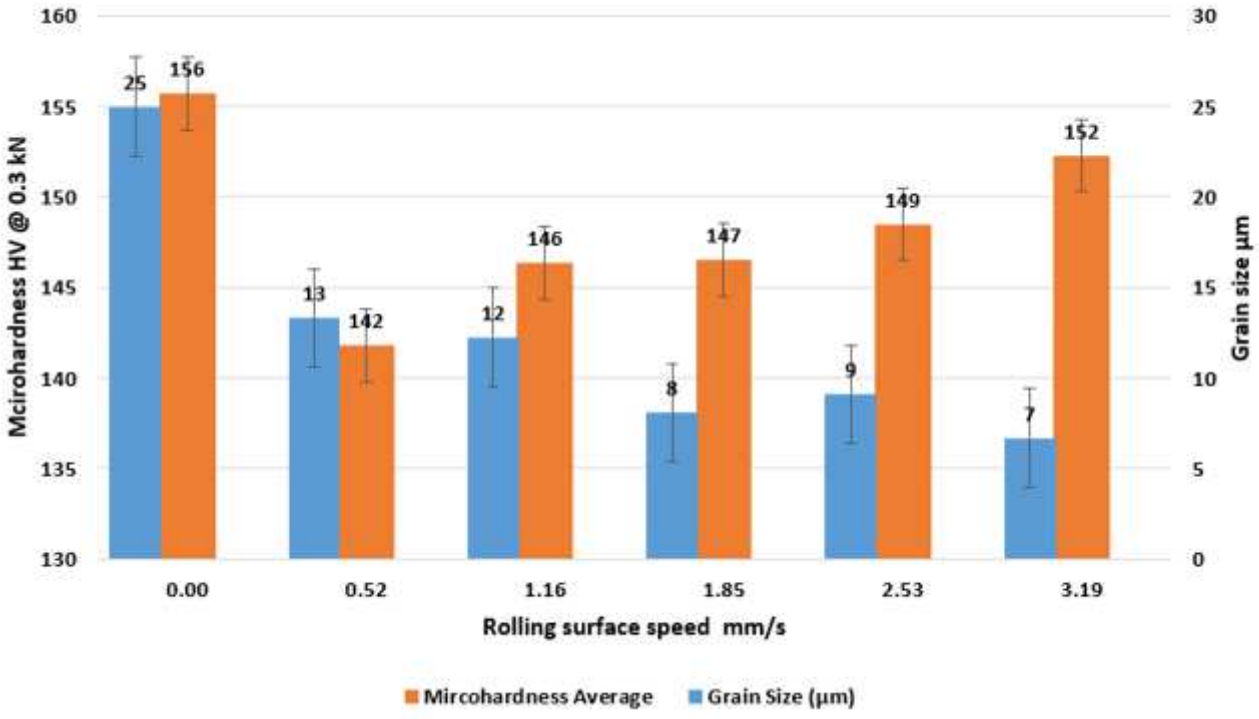

Figure 3

Effect of rolling surface speed on grain size and microhardness of CP-Ti wire during ISEPT.

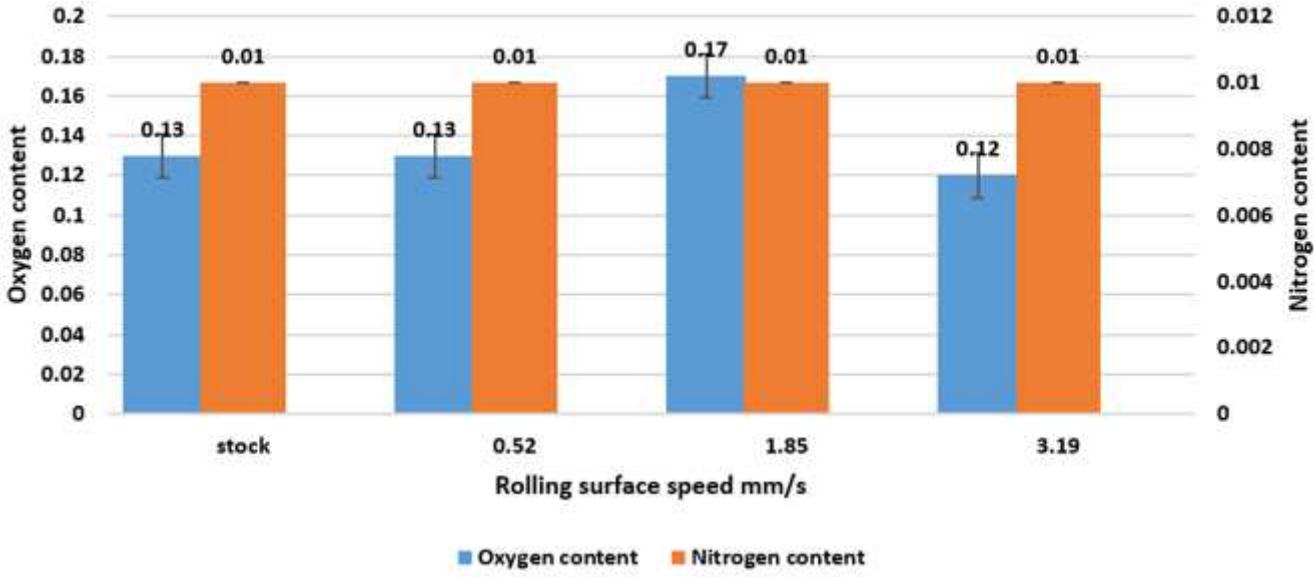

Figure 4

Effect of rolling surface speed on oxygen and nitrogen content of CP-Ti wire during ISEPT.

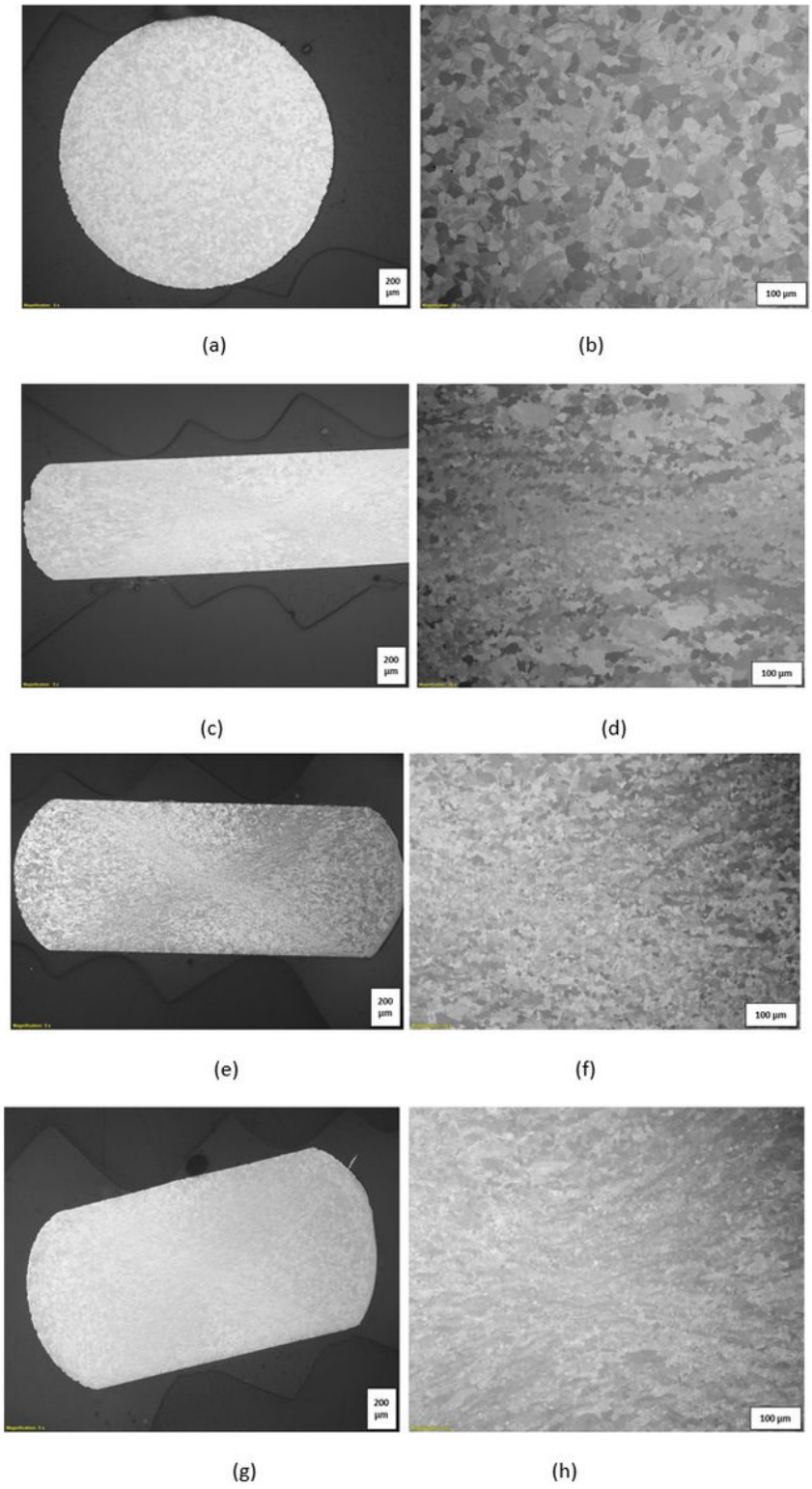

Figure 5

LM microstructures of CP-Ti wire cross section, (a,b) before ISEPT, (c,d) at 0.52 mm/s (e,f) at 3.19 mm/s and (g,h) at 6.4 mm/s RSS.

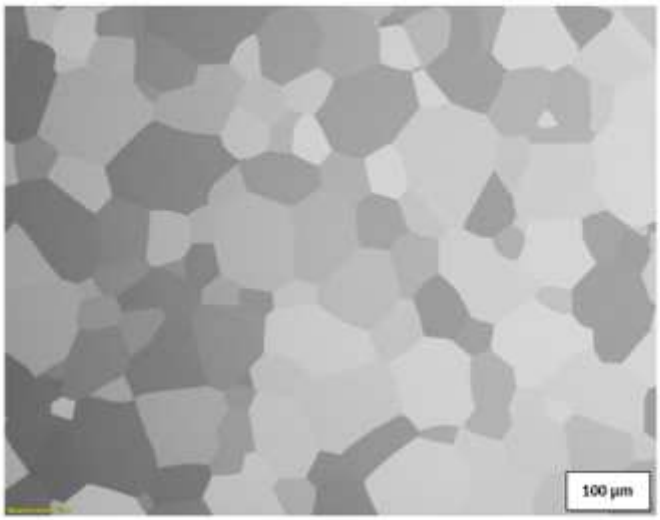

Figure 6

LM image of CP-Ti strip initial microstructure.

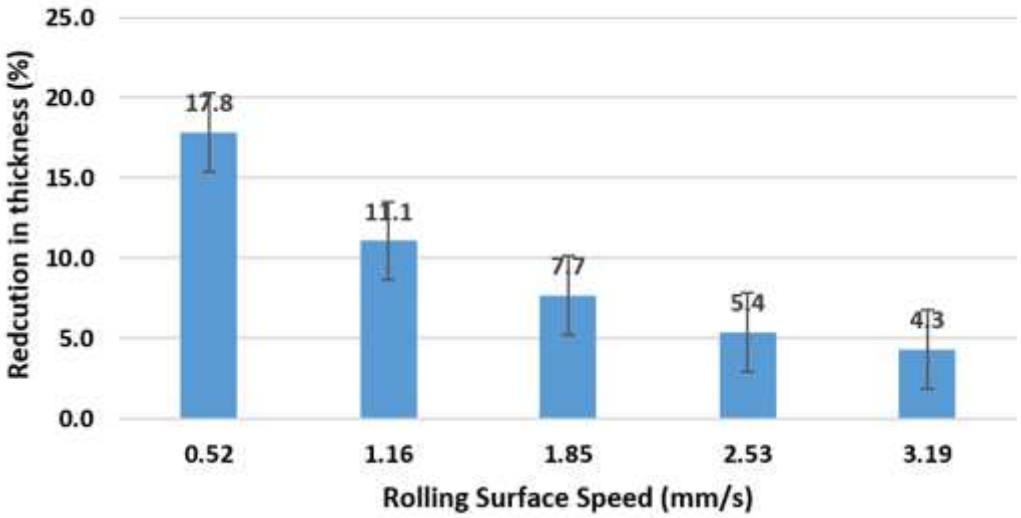

Figure 7

RSS as a function of reduction for electro-plastic treated 6.5×5 mm CP-Ti strip.

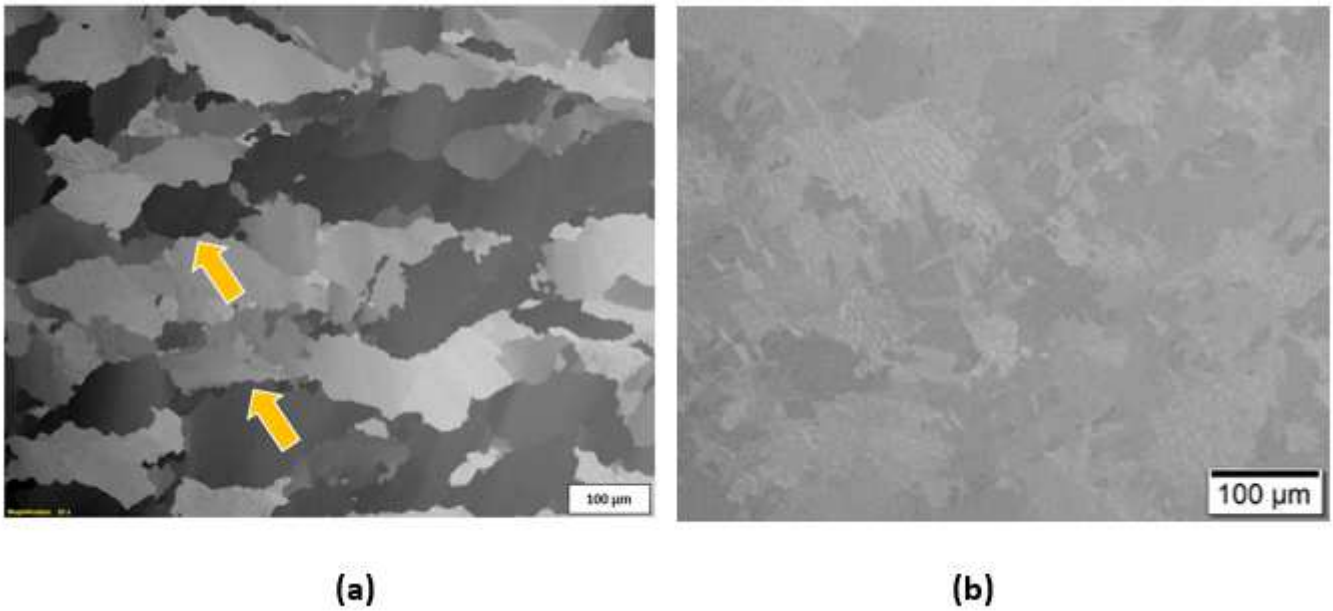

Figure 8

LM image of CP-Ti strip (a) at 0.52 mm/s RSS (arrows show grain boundary serration) and (b) at 1.16 mm/s RSS.

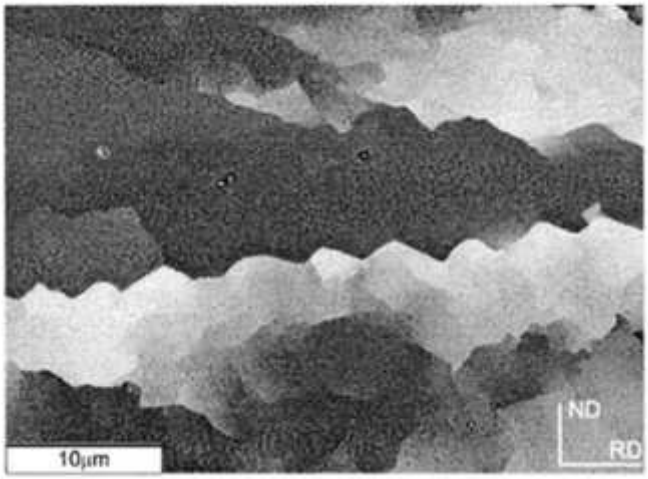

Figure 9

Grain boundaries serration as reported by Humphreys et al. [16].

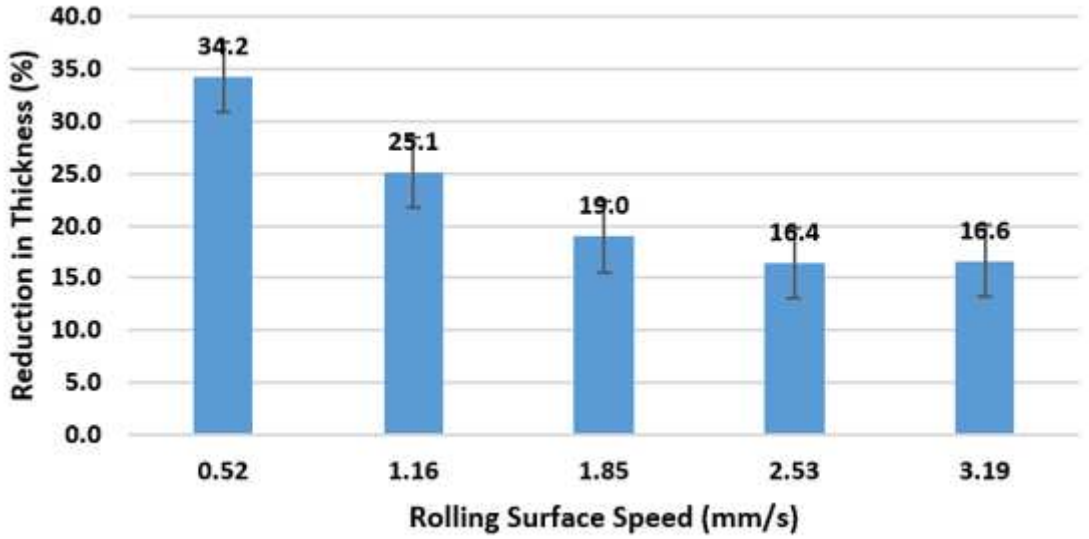

Figure 10

Effect of RSS on thickness reduction for 5×3 mm cross-section CP Ti strip at 1.5 kA and 0.7 MPa.

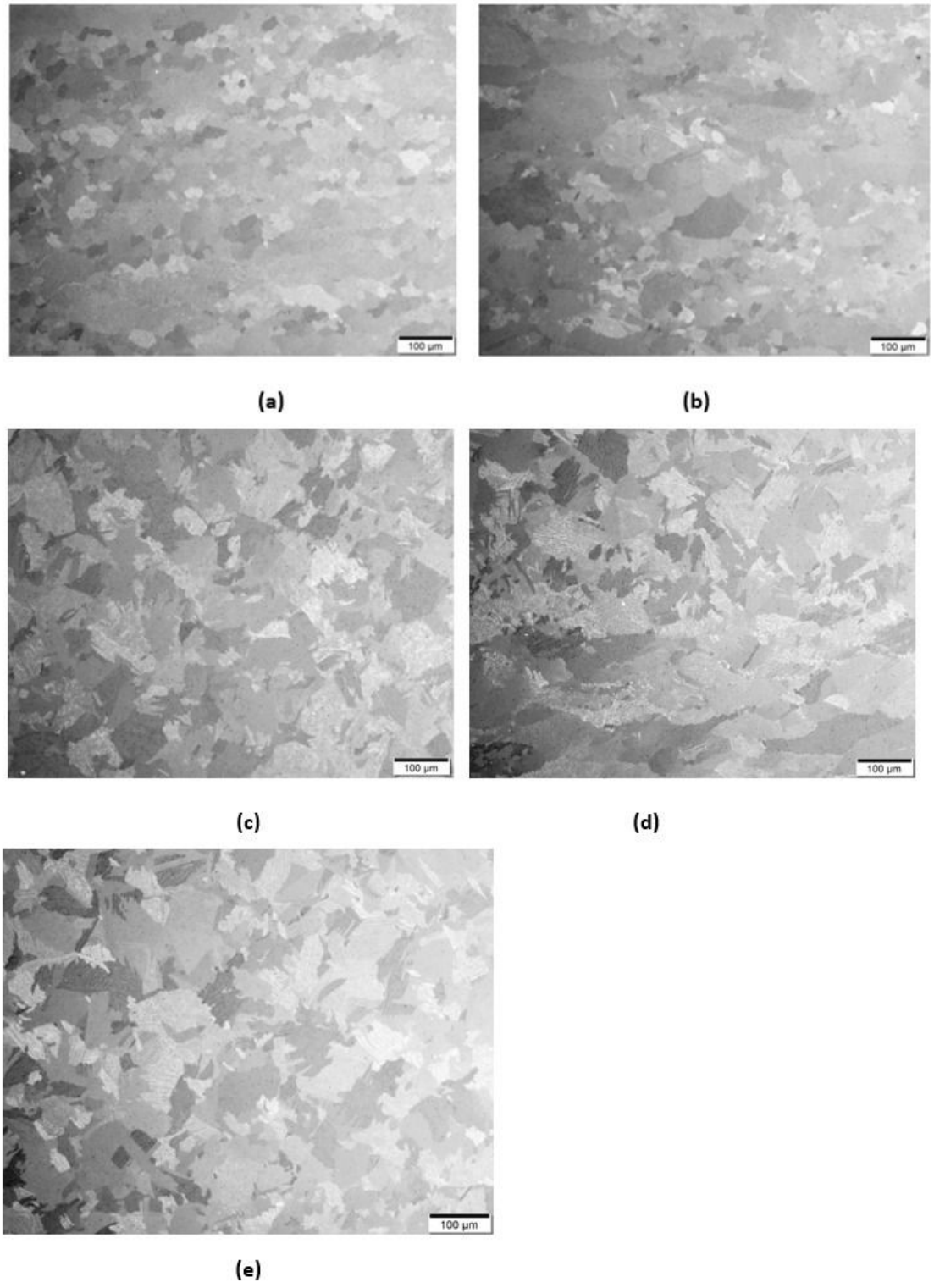

Figure 11

Microstructure (LM) images of the electro-plastically deformed 3×5 mm CP-Ti strips at 1.5 kA and 0.7 MPa corresponding to (a) 0.52mm/s, (b) 1.16 mm/s, (c) 1.85 mm/s, (d) 2.53 mm/s and (e) 3.19 mm/s RSS.

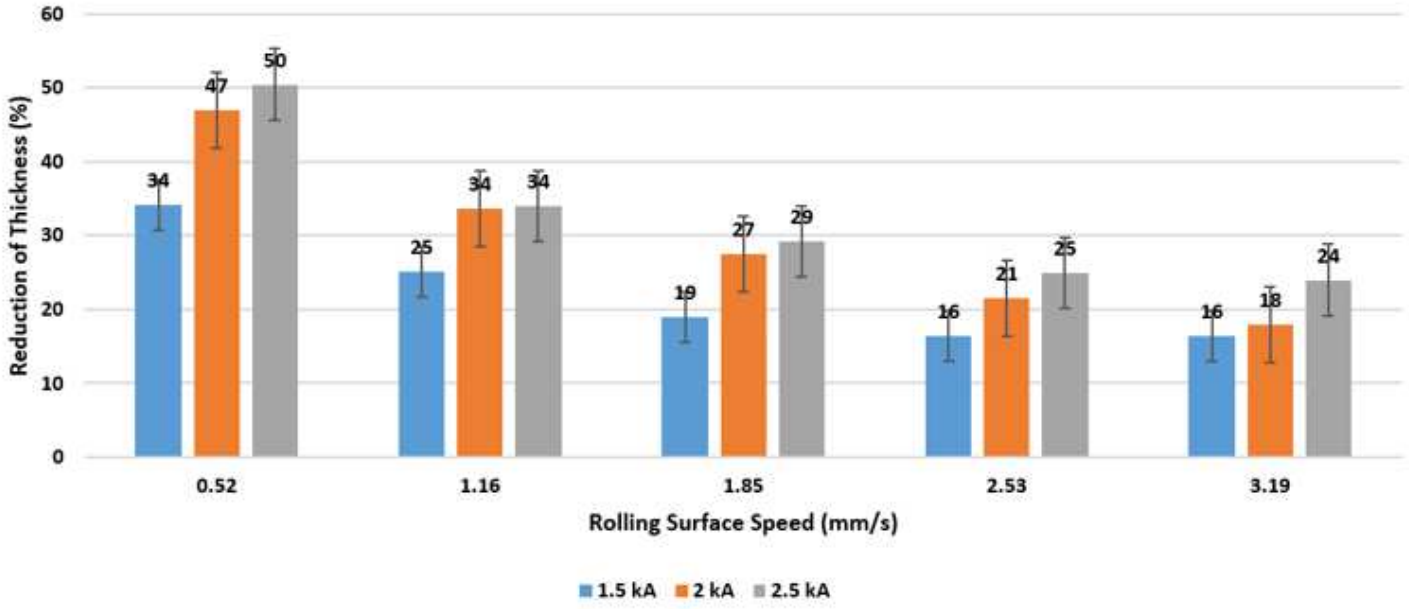

Figure 12

Effect of the applied current on ISEPT of a 5×3 mm CP Ti strip at a constant 0.7 MPa rolling pressure.

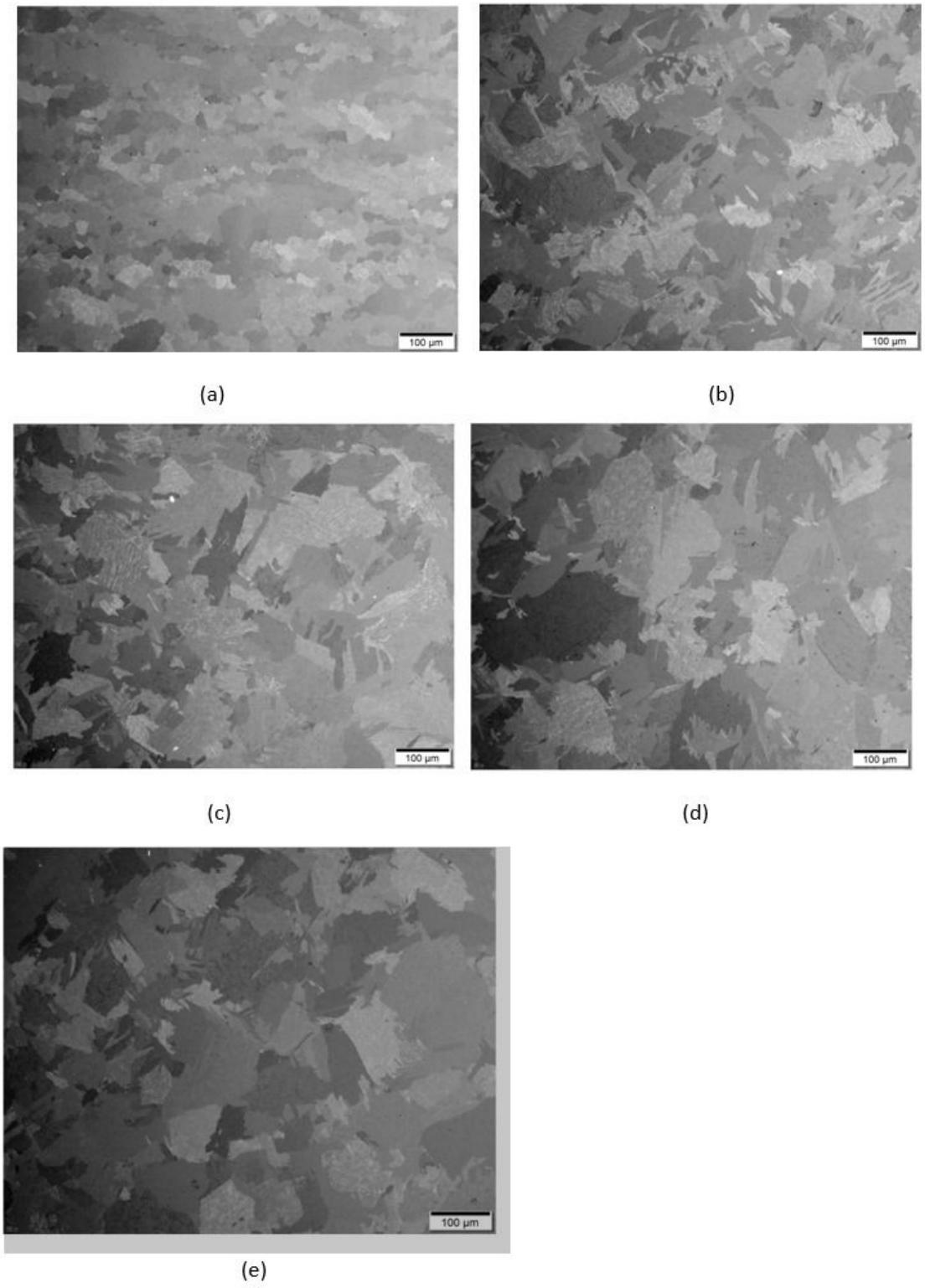

Figure 13

LM images of 3×5 mm CP-Ti strip microstructure after ISEPT at 2.0 kA and 0.7 MPa corresponding to (a) 0.52mm/s, (b) 1.16 mm/s, (c) 1.85 mm/s, (d) 2.53 mm/s and (e) 3.19 mm/s RSS.

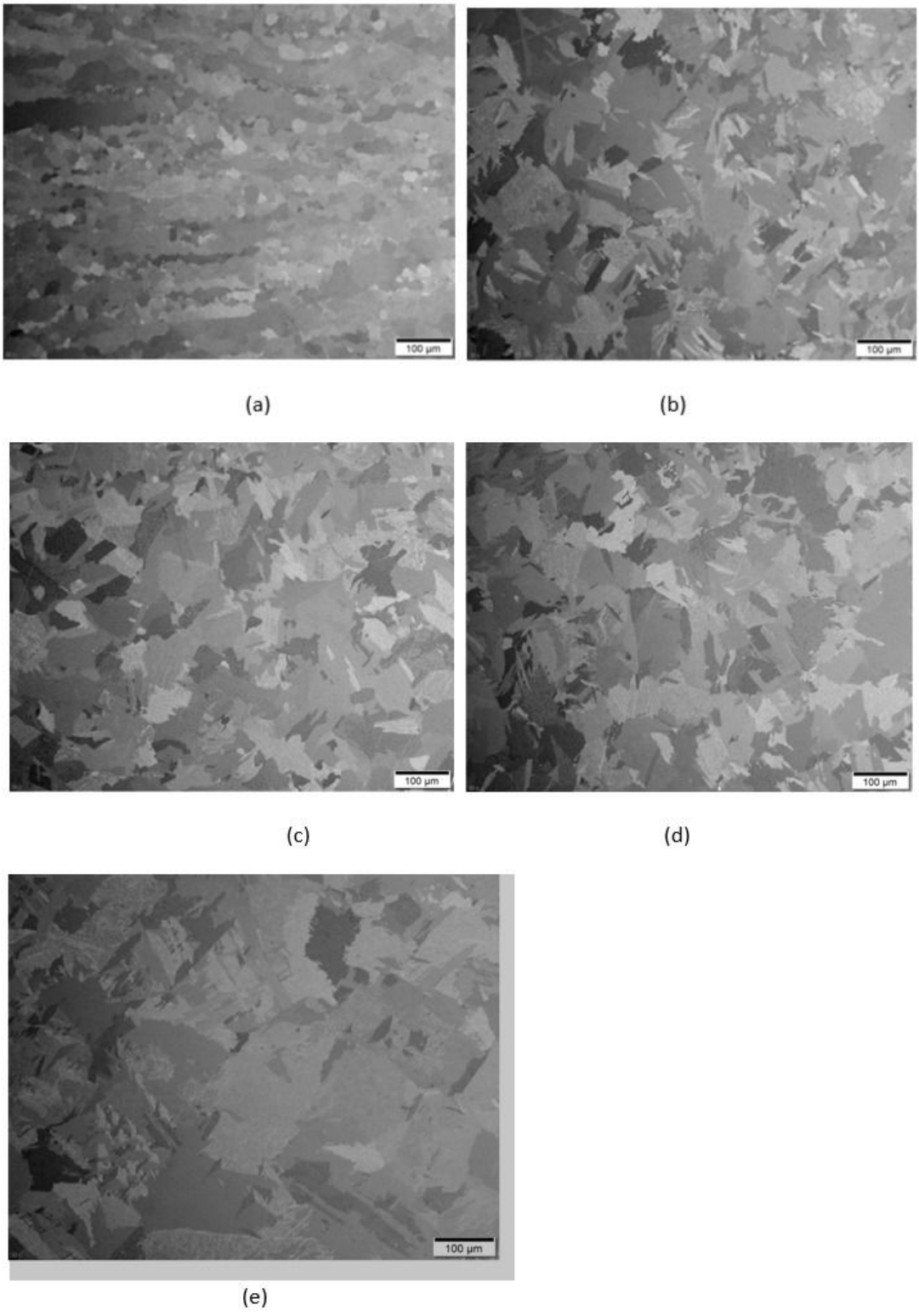

Figure 14

LM images of 3×5 mm CP-Ti strip microstructure after ISEPT at 2.5 kA and 0.7 MPa corresponding to (a) 0.52mm/s, (b) 1.16 mm/s, (c) 1.85 mm/s, (d) 2.53 mm/s and (e) 3.19 mm/s RSS.

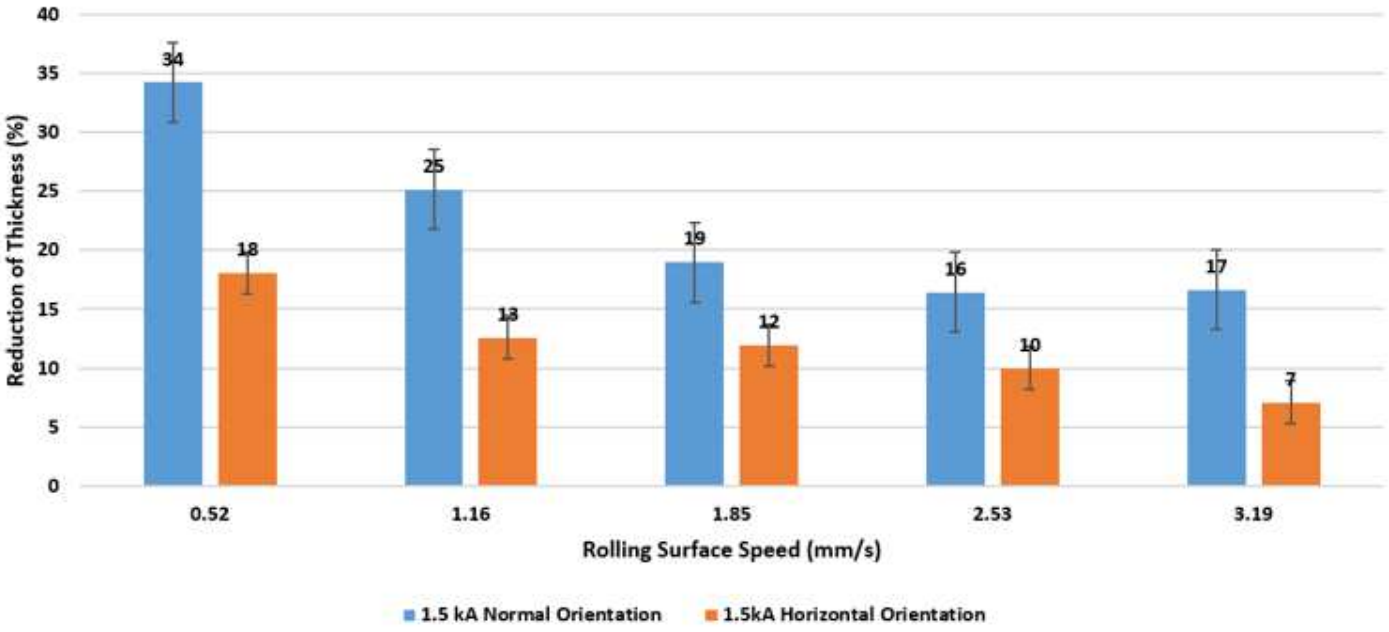

Figure 15

Effect of electro-plastic rolling orientation on the reduction of 5x3 mm CP Ti strip.

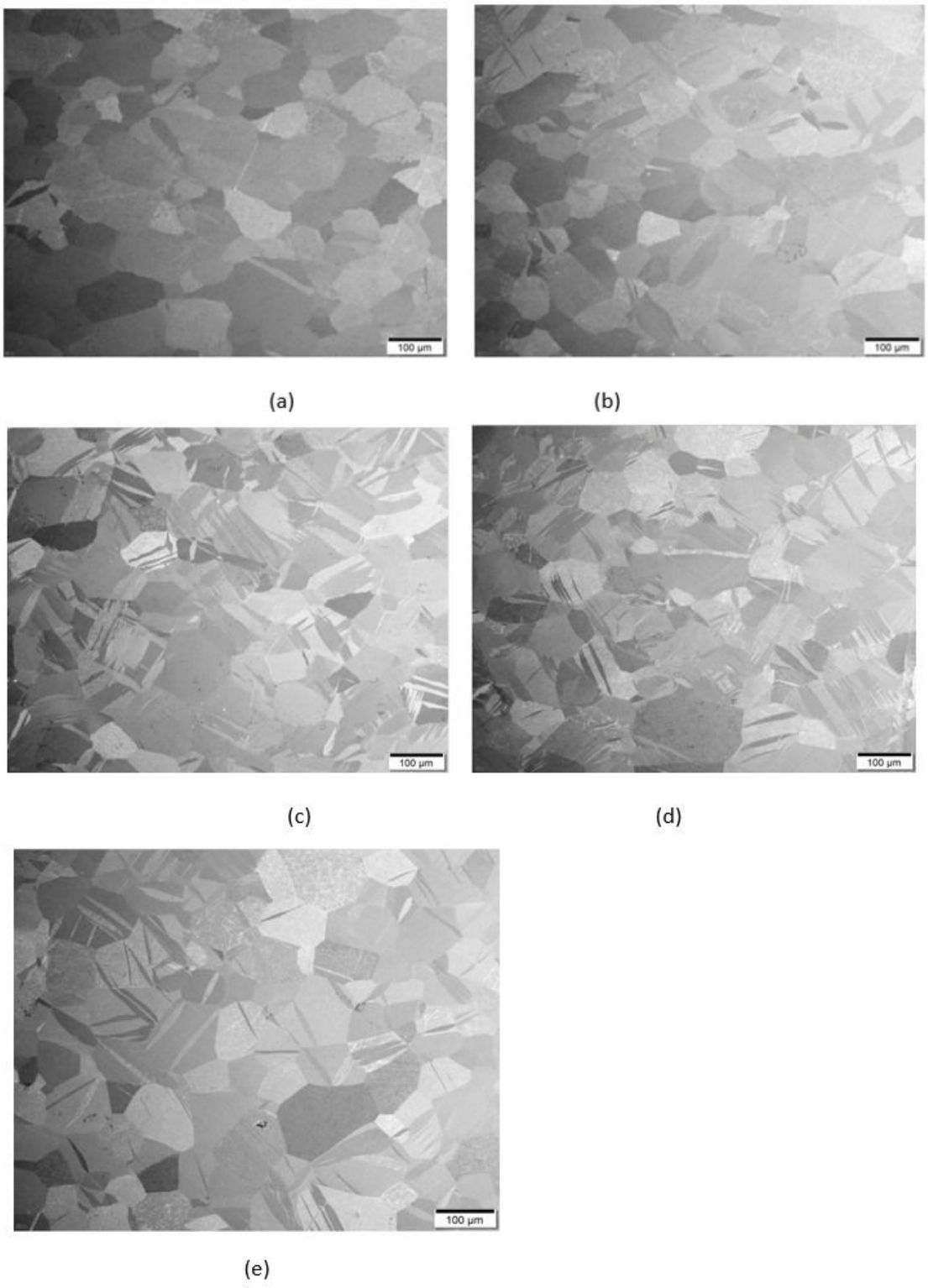

Figure 16

LM images of ISEPT 5×3 mm CP Ti strips deformed under horizontal orientation at (a) 0.52 mm/s, (b) 1.16 mm/s, (c) 1.85 mm/s, (d) 2.53 mm/s and (e) 3.19 mm/s RSS.

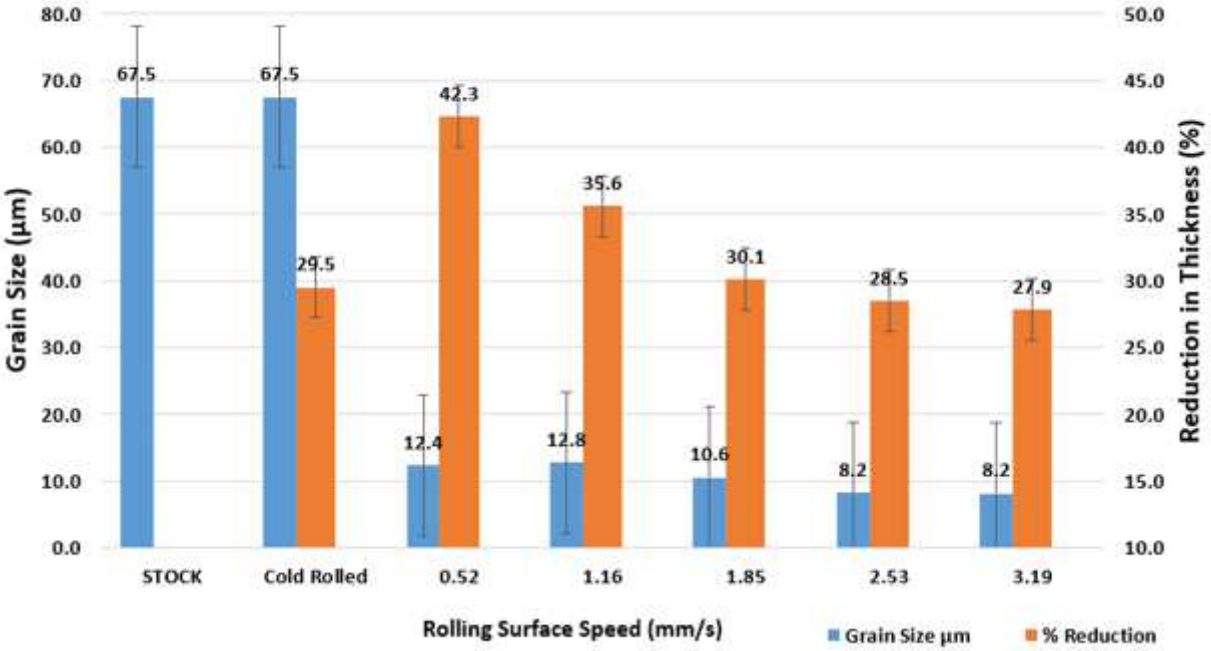

Figure 17

Grain size and reduction as a function of RSS for 30% cold worked, and electro-plastic treated strip processed at 1.5 kA and 0.7 MPa.

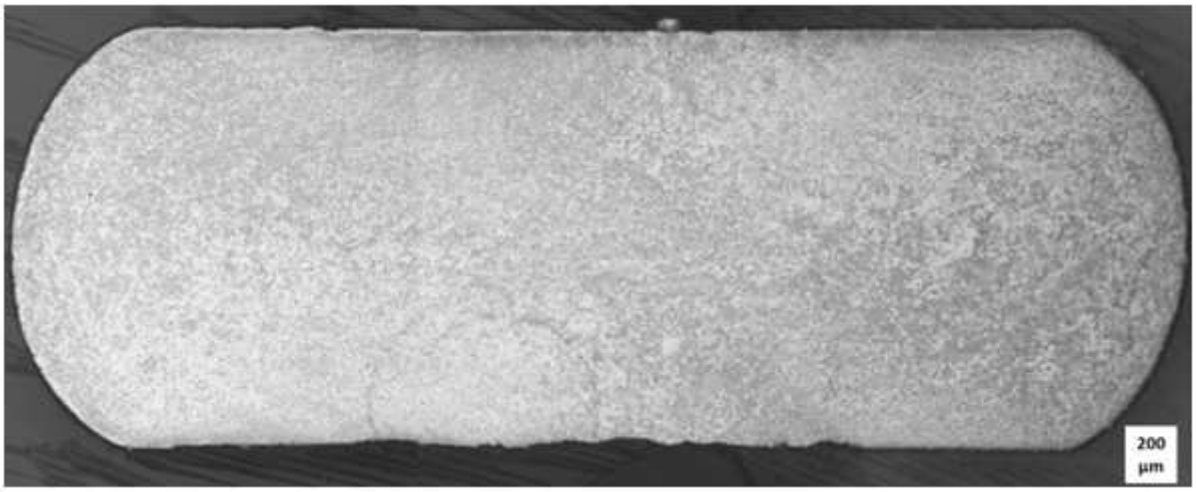

Figure 18

The low magnification microstructure (etched) of cold-worked and electro-plastic treated CP Ti strip at 1.5 kA, 0.7 MPa and 0.52 mm/s RSS, which is largely recrystallized.

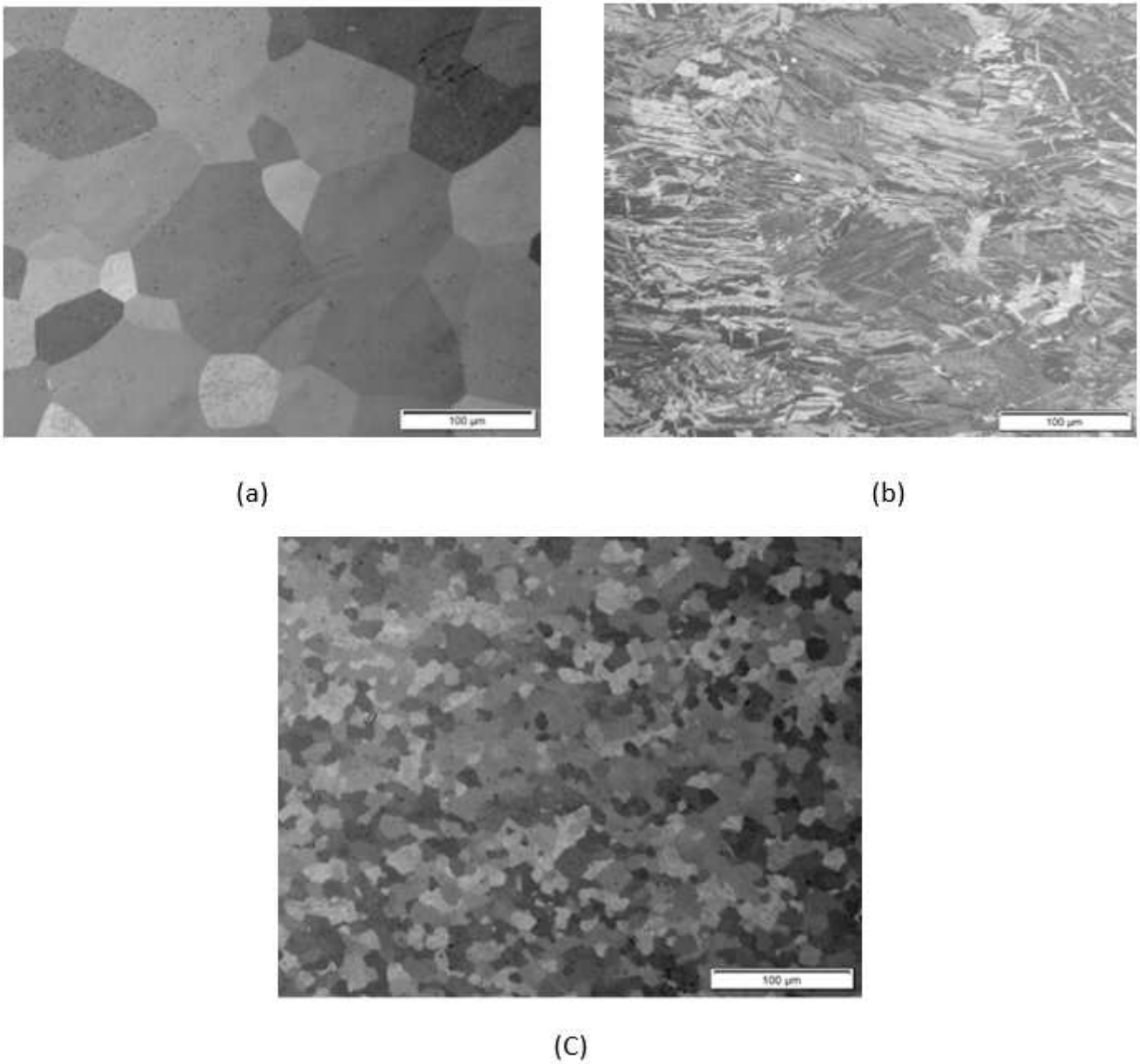

Figure 19

LM images of CP Ti strip (a) as received microstructure, (b) the microstructure after 30% cold working, (c) recrystallized after ISEPT at 1.5 kA, 0.7 MPa, and 0.52 mm/s.

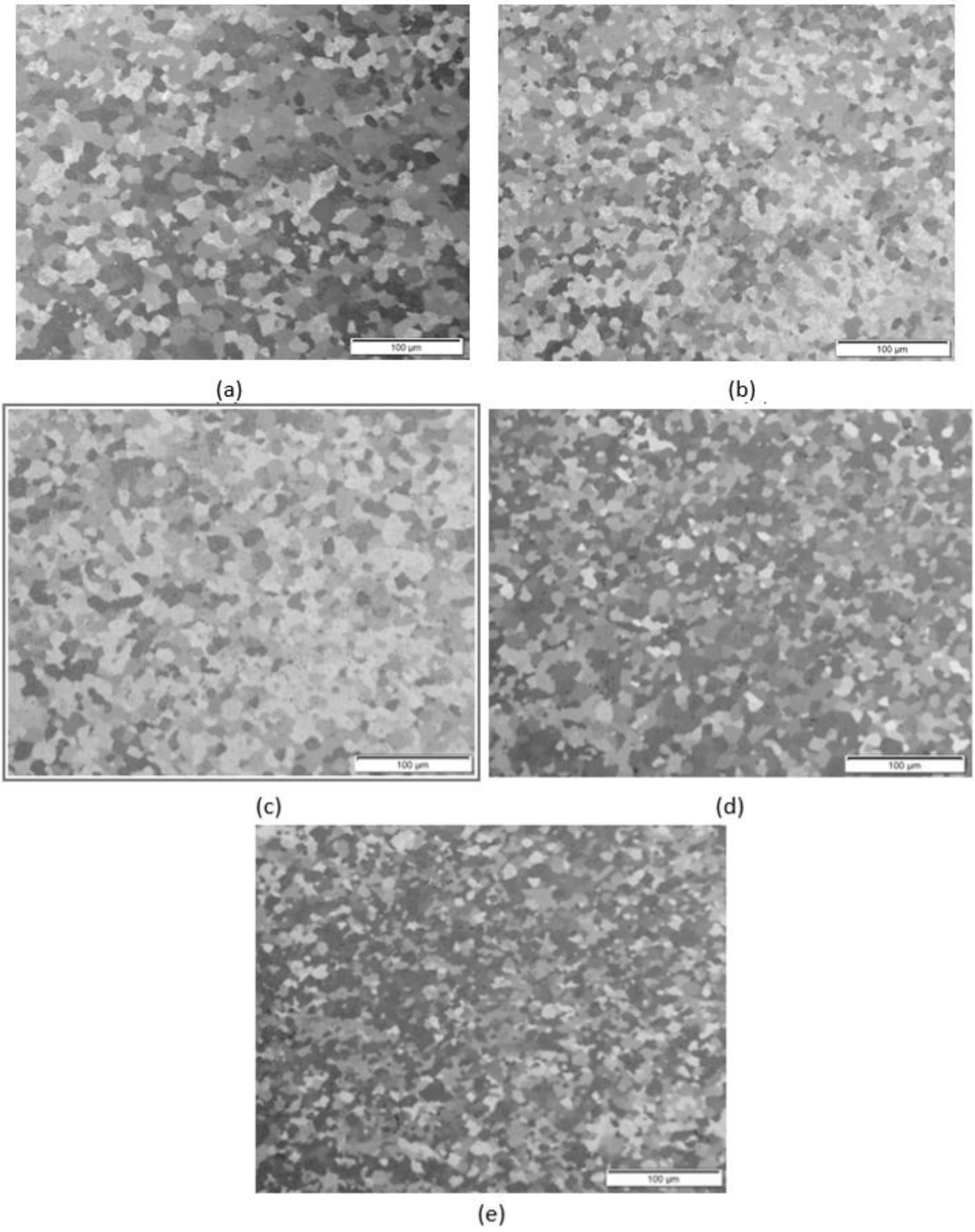

Figure 20

LM images of CP Ti microstructure that was cold rolled prior to ISEPT at 1.5 kA, 0.7 MPa and, (a) 0.52 mm/s, (b) 1.16 mm/s, (c) 1.85 mm/s, (d) 2.53 mm/s, (e) 3.19 mm/s RSS.

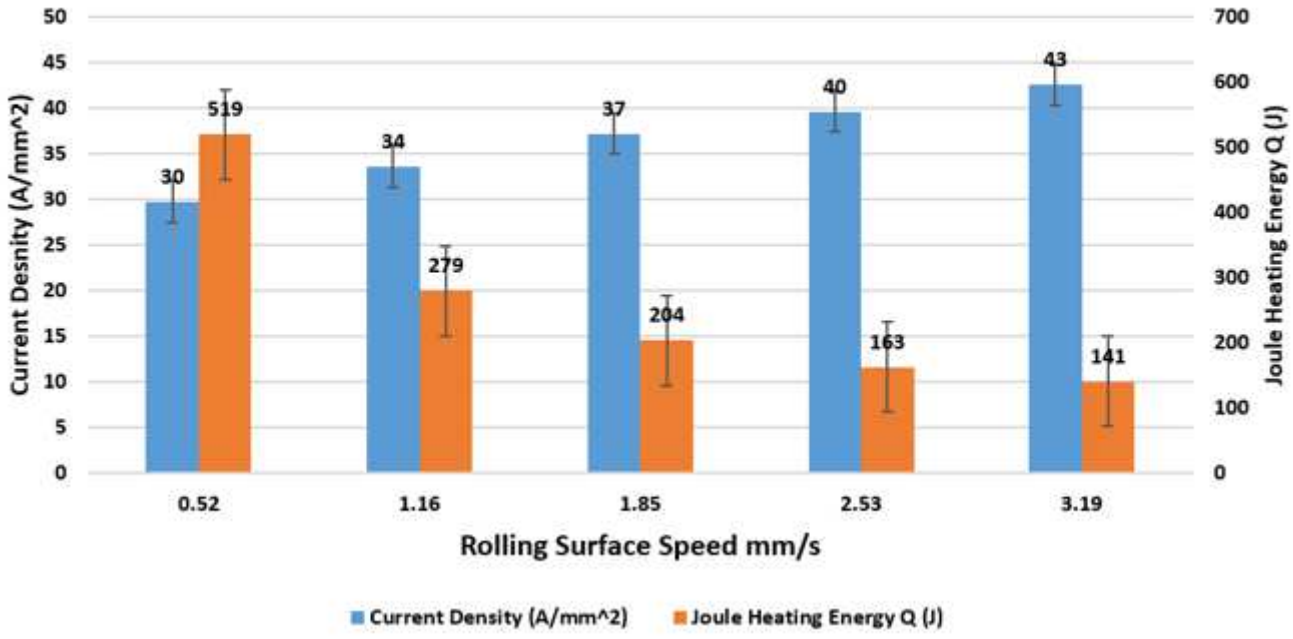

Figure 21

The current density and Joule heating energy as a function of RSS for in-situ electro-plastic processed CP Ti wire at 1.5 kA and 0.7 MPa.

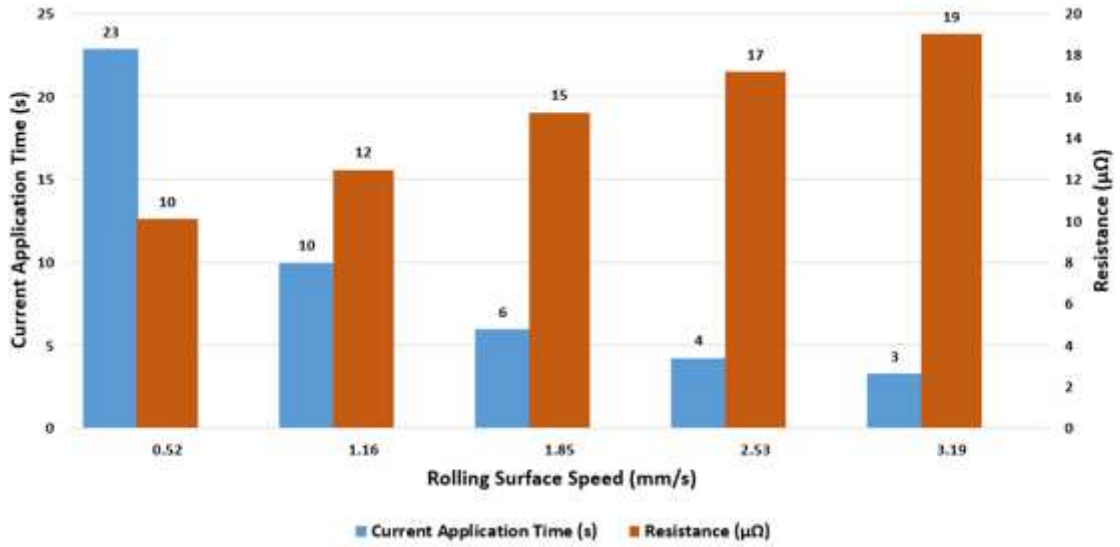

Figure 22

The estimated sample's resistance (μΩ) and current application time (s) as a function of RSS for CP Ti Wire.

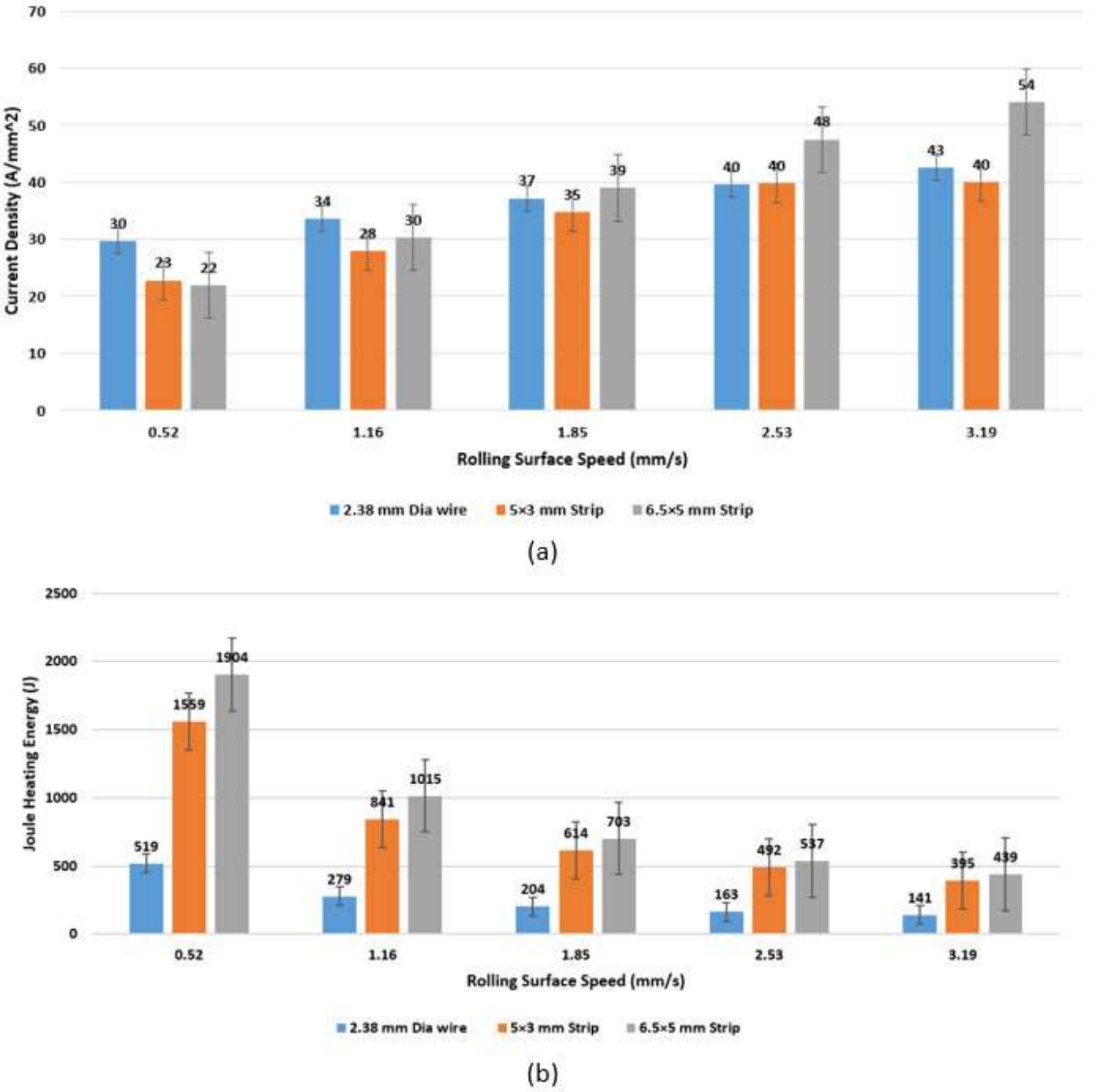

Figure 23

Comparison of the CP Ti electro-plastic deformation for 2.38 mm diameter wire, 5×3 mm strip, and 6.5×5 mm strip as a function of RSS at 1.5kA and 0.7 MPa (a) current density (A/mm2), and (b) Joule heating energy (J).

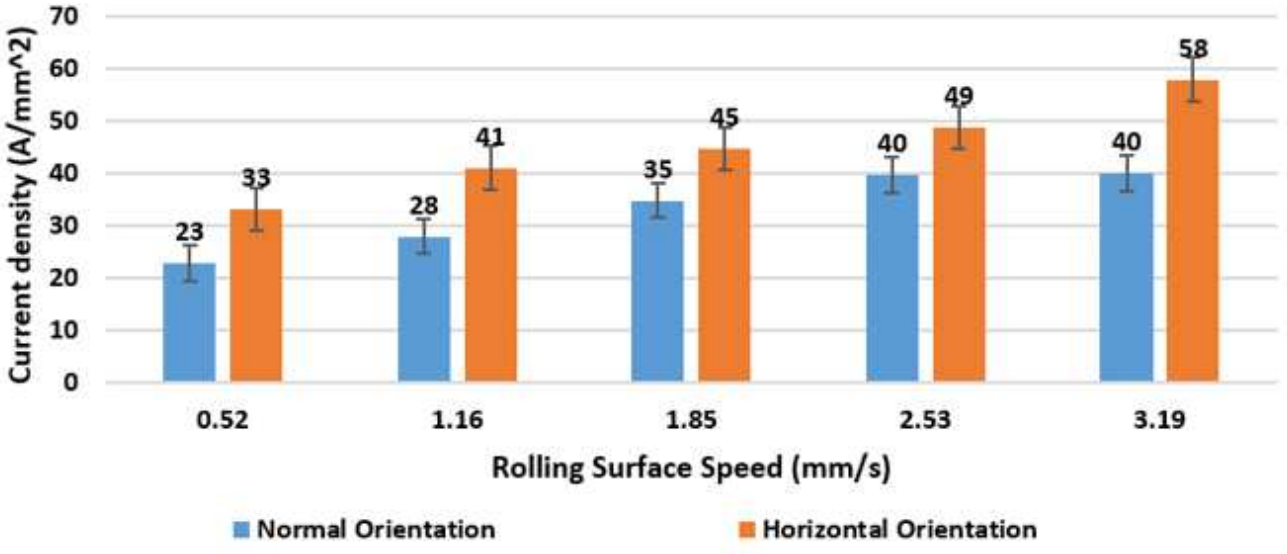

(a)

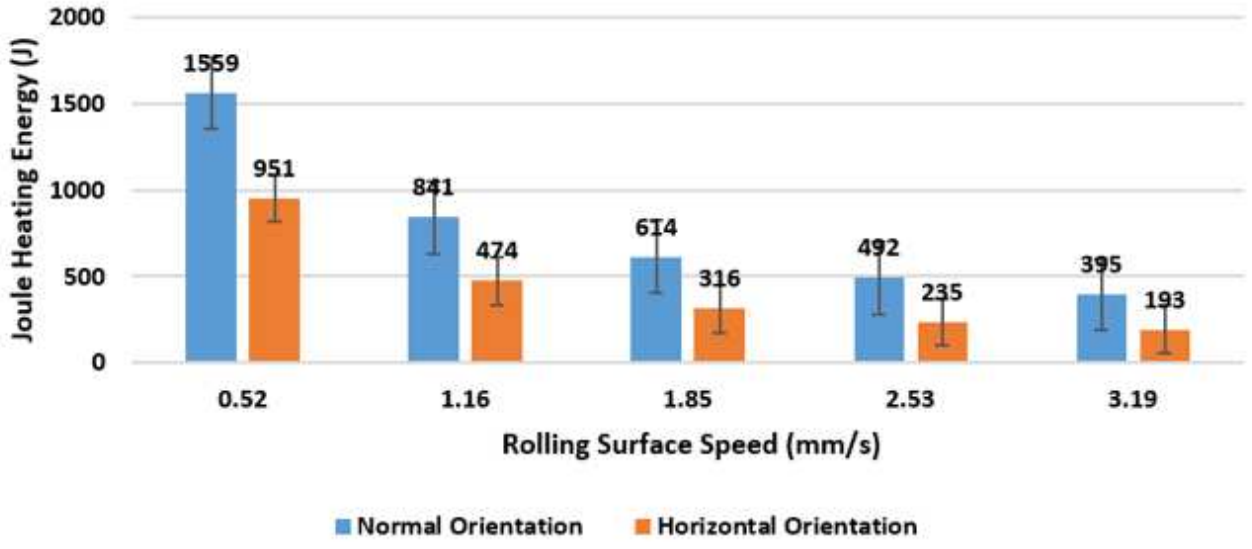

(b)

Figure 24

Current density (a) and Joule heating energy (b) as a function of RSS for the 5×3 cross-section CP Ti strips rolled in horizontal and vertical orientations.

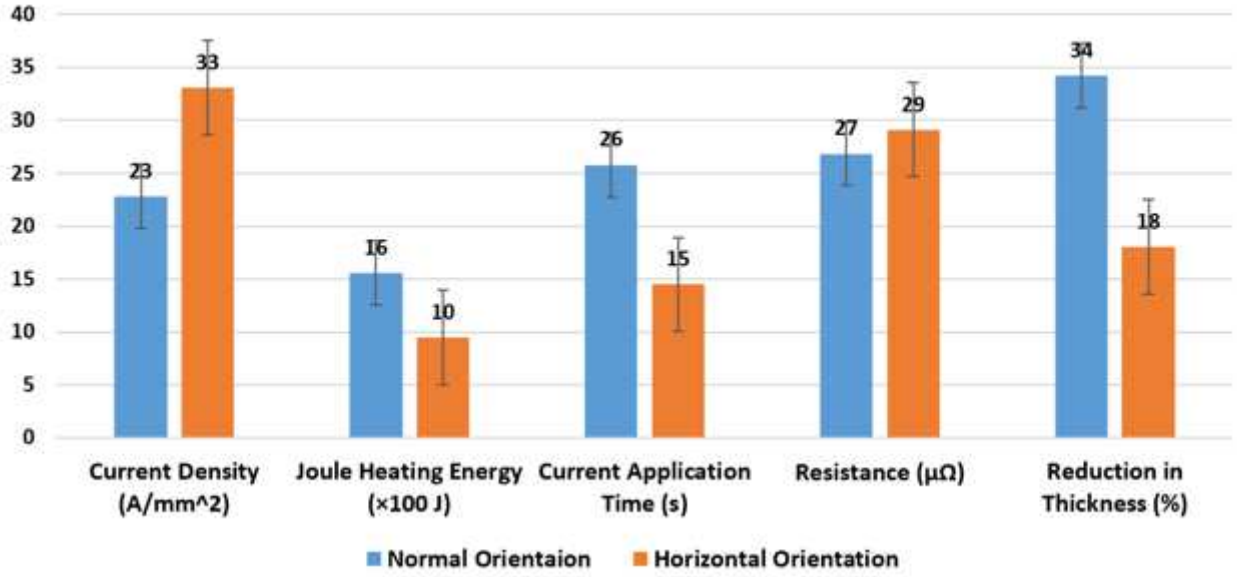

Figure 25

Comparison of the parameters for horizontal and Normal electro-plastic treated 5×3 mm CP Ti strips at 1.5 kA, 0.7 MPa and 0.52 mm/s RSS.

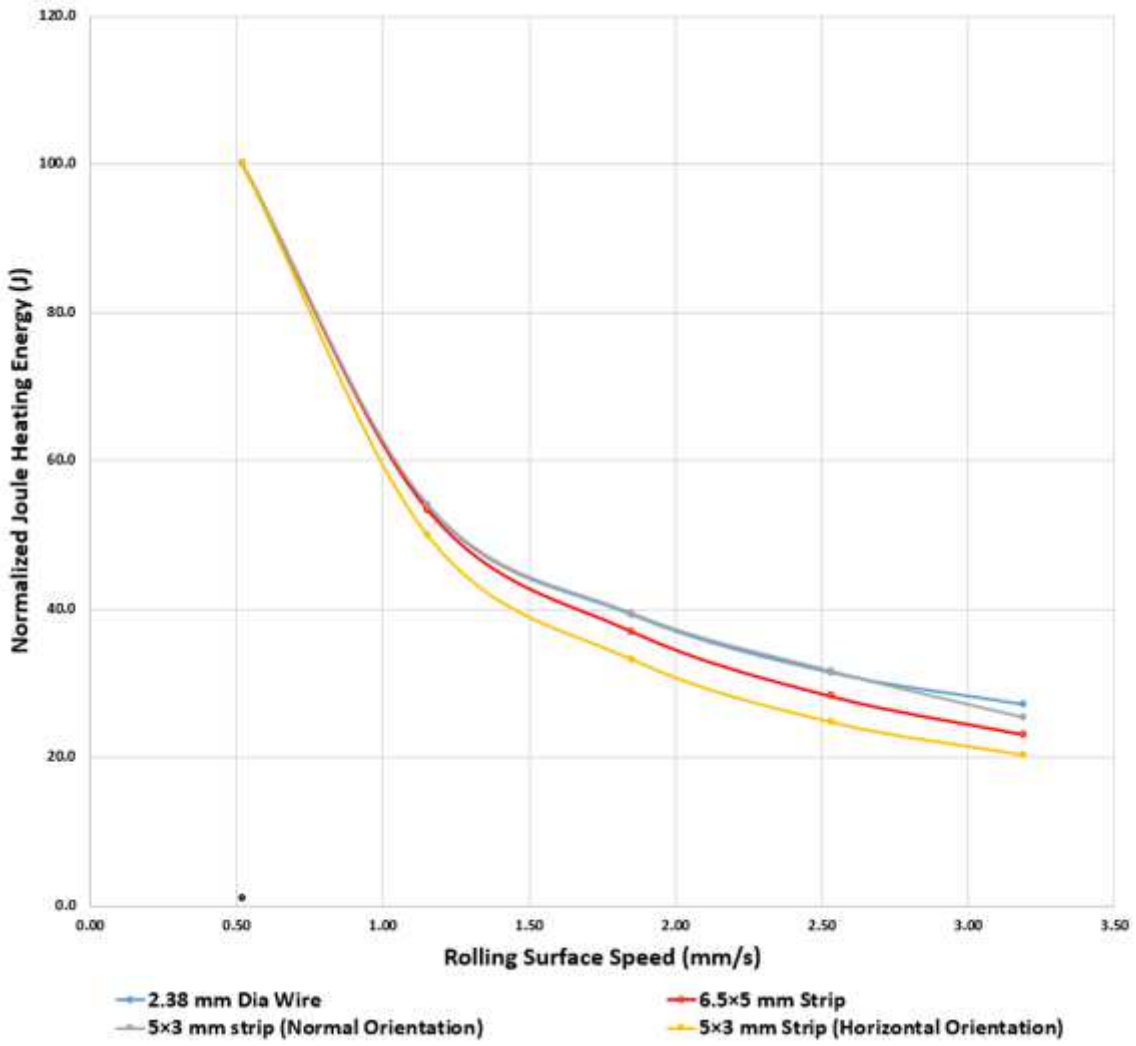

Figure 26

Normalized Joule heating energy for the ISEPT samples.